약학박사 학위논문

Effects of Tentonin3 / TMEM 150C on glucose-stimulated insulin secretion

Tentonin3 / TMEM150C가

포도당자극성 인슐린 분비에 미치는 영향 연구

2019년 2월

서울대학교 융합과학기술대학원

분자의학 및 바이오제약학과

위 정 원


VERI
LUX
TAS
MEA

약학박사 학위논문

Effects of Tentonin3 / TMEM 150C on glucose-stimulated insulin secretion

Tentonin3 / TMEM150C가 포도당자극성 인슐린 분비에 미치는 영향 연구

2019년 2월

서울대학교 융합과학기술대학원

분자의학 및 바이오제약학과

분자의학 및 바이오제약학 전공

위 정 원

Abstract

Glucose is a starting material for nearly all biosynthetic reactions in our body. Using glucose, cells generate adenosine triphosphate (ATP), the main source of energy in our body, through glycolysis and mitochondria. Excess glucose is stored as glycogen for future use. Not like other parts of the body, the brain cannot store glucose and mostly depends on the glucose in the bloodstream. Therefore, it is important to maintain a constant level of blood glucose, which process is known as glucose homeostasis. Glucose homeostasis is regulated mainly by pancreatic hormones. Food intake triggers a rise in blood glucose levels, which is monitored by pancreas. The pancreas releases a hormone, insulin, which brings glucose to the tissues for respiration or to the liver glycogenesis, in which the glucose is stored as glycogen. During the fasting state, the other hormone glucagon promotes hepatic glucose production (also known as glycogenolysis), which raises the dropped blood glucose level back to the normal range. Effects of both hormones are critical for the glucose homeostasis, but the homeostasis is mainly regulated by insulin.

Glucose-stimulated insulin secretion in β-cells is mediated through ATP-sensitive K^+ (K_{ATP})-dependent pathway. Once the cell detects high glucose in the plasma, glucose is transported into the cell via glucose transporter 2 (GLUT2) and metabolized by glycolysis

increasing the intracellular ATP/ADP ratio. This leads to the closure of K_{ATP} channels, which in turn depolarizes membrane potentials and activates voltage-gated Ca^{2+} channels (VGCC). Increased cytoplasmic Ca^{2+} level triggers Ca^{2+}-dependent exocytosis of insulin granules. Although the main triggering pathway for insulin secretion is K_{ATP} channel-dependent pathway, involvement of K_{ATP} channel-independent β- cell depolarization in response to high extracellular glucose level has been also proposed. One of candidate mechanisms for the latter pathway derived insulin secretion is that high glucose concentration not only depolarizes membrane potential of the β-cells via K_{ATP} channel, but also induces cell inflation, which process is described as swelling-stimulated insulin secretion. Many studies have shown that β-cell swelling, upon glucose or hypotonic stimulations, is sufficient to release insulin granules through ion channels such as volume regulated anion channels and/or stretch activated cation channels, that sense stretch of β-cell membrane and develop depolarization. Recently, the molecular identity of the anion channel was found to be SWELL1 (83), however, the molecular identity for the stretch-activated cation channel responsible for swelling-stimulated insulin secretion in β-cells remains unknown.

Recently our lab identified a new mechanosensitive cation channel, Tentonin 3 (TTN3/ TMEM150c), that mediates slowly adapting currents in various neurons. Interestingly, along with dorsal-root ganglia neuron, it is highly expressed in pancreas. In the present study, we

determined whether TTN3 plays a functional role in pancreas and possible involvement in the glucose-stimulated insulin secretion by mediating cation influx to hypotonic stimulation. We discovered that TTN3 is expressed in mouse pancreatic β-cells and mediates mechanosensitive responses. As glucose-induced swelling is a well-known mechanical stimuli in pancreas, we further assessed the activity of TTN3 to high glucose- or hypotonic-stimulations. Both of glucose- and hypotonic stimulations induced cationic currents in isolated pancreatic β-cells, and the response was significantly reduced in *Ttn3* KO β-cells. In addition, genetic ablation of *Ttn3* showed decreased electrical activity and Ca^{2+} influx in β-cells to those stimulations. Moreover, *Ttn3* KO mice showed impaired glucose tolerance with decreased insulin secretion *in vivo.* Here we propose that TTN3, as a stretch-activated cation channel, contributes to the glucose-stimulated insulin secretion in pancreatic β-cells.

Keywords:

Type 2 Diabetes (T2D); Tentonin3 (TTN3); Mechanosensation; Pancreatic β-cells; Stretch-activated cation channel (SAC); Glucose-stimulated insulin secretion (GSIS);

Student number: 2011-24248

Table of Contents

Abstract **1**

Table of Contents **4**

List of Figures **8**

Introduction **10**

1. Glucose Homeostasis **10**

1.1. Overview 10

1.2. Glucose Production 10

1.3. Glucose Utilization 11

1.4. Significance of Glucose Homeostasis 11

1.5. Regulation of Glucose Homeostasis 12

1.5.1. Pancreas 12

1.5.2. Hormonal regulation of glucose homeostasis 13

2. Diabetes Mellitus 18

2.1. Overview 18

2.2. Symptoms 19

2.3. Classification of Diabetes Mellitus 19

2.3.1. Type 1 Diabetes (T1D) 19

2.3.2. Type 2 Diabetes (T2D) 19

2.3.3. Gestational diabetes mellitus (GDM) 20

2.3.4. Other types 20

3. Mechanisms of Insulin Secretion 20

3.1. Overview 20

3.2. Electrical activity in pancreatic β-cells 21

3.3. K_{ATP}–channel dependent pathway 21

3.4. K_{ATP}–channel independent pathway 24

3.4.1. Swelling-stimulated insulin secretion....24
4. Mechanotransduction....26
4.1. Overview....26
4.2. Mechanically gated ion channels....26
4.3. Mechanosensitivity of pancreatic β-cells....26
4.3.1. Volume-regulated anion channels....27
4.3.2. Stretch-activated cation channels....28
5. Tentonin3....28
5.1. Overview....28
5.2. Function....30
5.3. Expression profile....30
Purpose of the study....32
Methods....33
1. Animals....33
2. Immunohistochemistry....33
3. RNA interference....34
4. RT-PCR....34
5. Primary culture of pancreatic β-cells....35
6. Cell Culture....35
7. Calcium Measurements....36
8. Electrophysiology....37
9. Solutions....37
10. Mechanical Stimulation....38
11. Glucose Tolerance Test....39
12. Insulin Tolerance Test....39
13. Insulin Secretion Assay....39
14. Statistics....40

Results.....41

1. The expression of TTN3 in pancreatic β-cells.....41

2. Primary cell culture of β-cells from *Ttn3* KO mouse.....43

2.1. TTN3 systemic KO mouse.....43

2.2. Islet morphology of WT and *Ttn3* KO mice.....43

2.3. Isolation of pancreatic islets.....43

2.4. Expression of TTN3 in mouse pancreatic islets and β-cell line.....44

3. TTN3 conducts mechanosensitive responses in mouse pancreatic β-cells.....49

4. TTN3 is activated by hypotonicity-induced swelling.....52

4.1. Overview.....52

4.2. Activation of TTN3 by hypotonicity induced swelling in HEK 293T cells.....52

4.3 Activation of TTN3 by hypotonicity induced swelling in isolated pancreatic β-cells.....53

5. TTN3 is activated by high glucose-induced swelling.....57

6. TTN3 activation contributes to the glucose-evoked depolarization of β-cells.....59

7. TTN3 activation contributes to the swelling-evoked depolarization in β-cells.....62

8. TTN3 evokes Ca^{2+} influx to glucose stimulation.....65

8.1. Calcium and Exocytosis.....65

8.2. TTN3-mediated Ca^{2+} influx in β-cell line, NIT-1.....65

8.3. TTN3-mediated Ca^{2+} influx to glucose stimulation in β-cells.....66

8.4. TTN3-mediated Ca^{2+} influx to hypotonic stimulation in β-cells.....66

9. TTN3-mediated Ca^{2+} influx and other pathways.....73

9.1. K_{ATP} channel-mediated Ca^{2+} influx.....73

9.2. VRAC channel 73

10. Impaired glucose tolerance and insulin secretion in *Ttn3* KO mice 76

10.1. TTN3-mediated insulin secretion in NIT-1 cells. 76

10.2. *Ttn3* KO mice show higher blood glucose level upon glucose stimulation. 76

10.3. Insulin sensitivity is preserved in *Ttn3* KO mice. 77

10.4. Decreased insulin secretion in *Ttn3* KO mice. 77

10.5. Role of TTN3 in Diabetic disease models. 78

Discussion 85

Conclusion 91

References 92

국 문 초 록 102

List of Figures

Figure 1. Cross section of the pancreas.....14

Figure 2. Homeostatic regulation of blood glucose level 15

Figure 3. The mechanism of glucose-stimulated insulin secretion from the β-cells.....23

Figure 4. Mechanism of swelling-induced insulin secretion in β-cells .25

Figure 5. Slowly activating mechanosensitive currents evoked by TTN3 29

Figure 6. Expression profiles of TTN3 genes 31

Figure 7. Immunofluorescence analysis of TTN3 in mouse pancreas 42

Figure 8. Schematic illustration of constitutive *Ttn3* KO mouse.....45

Figure 9. Islet morphology of *Ttn3* KO mice 46

Figure 10. Isolation of mouse pancreatic islets.....47

Figure 11. Immunofluorescence analysis of single pancreatic β-cell ..48

Figure 12. Mechanosensitive currents in β-cells 50

Figure 13. TTN3 activation by swelling in HEK293T cells 54

Figure 14. TTN3 activation by swelling in pancreatic β-cells 56

Figure 15. TTN3 activation by glucose in pancreatic β-cells.....58

Figure 16. Electrical activities to glucose stimulation in β-cells.....60

Figure 17. Analysis of electrical activities to glucose stimulation 61

Figure 18. Electrical activities to hypotonic stimulation in β-cells.....63

Figure 19. Analysis of electrical activities to hypotonic stimulation 64

Figure 20. Glucose-stimulated Ca^{2+} influx in NIT-1 cells.....68

Figure 21. Swelling-stimulated Ca^{2+} influx in NIT-1 cells 69

Figure 22. Knockdown of TTN3 in β-cell line, NIT-1 70

Figure 23. Glucose-stimulated Ca^{2+} influx in pancreatic β-cells.....71

Figure 24. Swelling-stimulated Ca^{2+} influx in pancreatic β-cells.....72

Figure 25. TTN3 mediates Ca^{2+} influx, independent of K_{ATP}-channel in response to glucose stimulation.....74

Figure 26. TTN3 mediates Ca^{2+} influx, independent of VRAC-channel in response to hypotonic stimulation.....75

Figure 27. Measurement of insulin secretion in NIT-1 cells.....79

Figure 28. *Ttn3* KO mice show higher blood glucose level.....80

Figure 29. Sensitivity to Insulin is preserved in *Ttn3* KO mice.....81

Figure 30. Decreased insulin secretion in *Ttn3* KO mice.....82

Figure 31. Effects of HFD on body weight in *Ttn3* KO mice.....83

Figure 32. Time course of food intake and water intake during HFD..84

Figure 33. Mechanism of swelling-stimulated insulin secretion in β-cells through TTN3.....89

Figure 34. Immunofluorescence analysis of Piezo1 in mouse pancreas 90

Introduction

1. Glucose Homeostasis

1.1. Overview

Our body needs energy to function, and the energy comes from the food we eat. Glucose, which comes from an ancient Greek word *gleukos*, meaning “sweet”, refers to a type of sugar (2). It is also called blood glucose as it travels through bloodstream to cells throughout the body (3).

1.2. Glucose Production

The body derives glucose from three different sources; dietary sources, the product of the breakdown of glycogen (glycogenolysis), or the synthesis of glucose from other carbon compounds (gluconeogenesis) (4). After food intake, the carbohydrates in the food we eat are digested in the stomach into monosaccharides such as galactose, fructose and glucose. Among them glucose constitutes 80 percent of monosaccharides (5). Transferred down into small intestine, glucose is absorbed by absorptive cells. Excess glucose is stored in liver as glycogen or converted to triglycerides and stored in adipose tissue (6). During the early phase of starvation, glycogenolysis in the liver or muscle cells is the primary source of glucose. Drop of blood glucose level, adrenal gland secretes epinephrine (adrenaline), growth hormone

and cortisol (7). Upon the stimulation by epinephrine, hepatocytes in the liver activate glycogen breakdown and release glucose into the bloodstream (8). Over longer periods of fasting, our body depends on the gluconeogenesis in the liver or kidneys. Glucose is synthesized from non-carbohydrate precursors such as lactate, glycerol, amino acids (9).

1.3. Glucose Utilization

Cells use glucose to create energy through glycolysis (anaerobic respiration) and/or pyruvate oxidation (anaerobic respiration). Glycolysis is the first pathway in cellular respiration and takes place in the cytoplasm of the cell. It breaks down 1 glucose molecule and produces 2 pyruvate molecules and 2 adenosine triphosphate (ATP) (10). The pyruvate generated by glycolysis is oxidized in the aerobic respiration that takes place in the mitochondria. The mitochondria uses oxygen to burn the pyruvate into heat and ATP, which is the major energy molecule of the cell (7). The organs accounting most of glucose uptake in our body are as follows: the brain (45-60%), skeletal muscle (15-20%), blood cells (5-10%), splanchnic organs (3-6%), and adipose tissue (2-4%) (11).

1.4. Significance of Glucose Homeostasis

The brain relies almost exclusively on glucose for its source of energy, as ATP is critical for neuronal and non-neuronal cellular maintenance, as well as the generation of neurotransmitters (12, 13). Unlike other parts of the body which store glucose as fat or glycogen,

the brain cannot store glucose more than a few minutes- supply, so it is critical for brain to receive a continuous supply of glucose through bloodstream. (4, 14)

1.5. Regulation of Glucose Homeostasis

Blood glucose levels fluctuate according to the status of our body, which is monitored by pancreas. The concentration of blood glucose drops to 50 mg/dl, when prolonged fasting, and rises up to 165 mg/dl after food intake in a healthy man. However, tightly regulated glucose homeostasis in our body maintains the average value within a narrow range, 70 ~ 110 mg/dl (4, 6).

There are many factors regulating the concentration of blood glucose; hormones, the sympathetic nervous system activity as well as the concentration of other nutrients, and exercise which may affect the sensitivity to hormones (4).

1.5.1. Pancreas

The pancreas is an abdominal organ located behind the stomach. The pancreas is made up of two kinds of glands with two primary functions; exocrine gland and endocrine gland as shown in Figure 1 (15). As an exocrine gland, acinar cells or exocrine cells in the pancreas regulates macronutrient digestion by releasing digestive enzymes such as amylase, pancreatic lipase and trypsinogen, into the ducts (16). In contrast, as an endocrine gland, four specialized cell

types, glucagon producing α-cells, amylin-, C-peptide- and insulin-producing β-cells, pancreatic polypeptide (PP)-producing γ-cells, and somatostatin-producing δ-cells, organized into a compact islet called an islet of Langerhans, secrete hormones into bloodstream and maintains glucose homeostasis (15). Changes in concentration of blood is monitored by the pancreas through its various hormones, the pancreas maintains blood glucose level within a narrow range (16).

1.5.2. Hormonal regulation of glucose homeostasis

The concentration of glucose in the bloodstream is mainly regulated by hormones by conducting storage and the utilization of glucose as required (6). The pancreas, after monitoring the blood glucose levels, secrete glucose regulatory hormones including insulin, glucagon, amylin, glucagon-like peptide-1 (GLP-1), gastric inhibitory polypeptide (GIP), epinephrine, cortisol, and growth hormones to maintain normal levels (17). Among them, the role of glucagon and insulin plays a key role in glucose homeostasis as described in Figure 2. In the fed state, the pancreas releases insulin which delivers glucose to the tissues for respiration or promotes glycogen synthesis in the liver and muscle and lipid formation in adipocytes. During the fasting state, however, the pancreas releases another hormone, glucagon, which stimulates hepatic glucose production from glycogen breakdown and lipolysis (18).

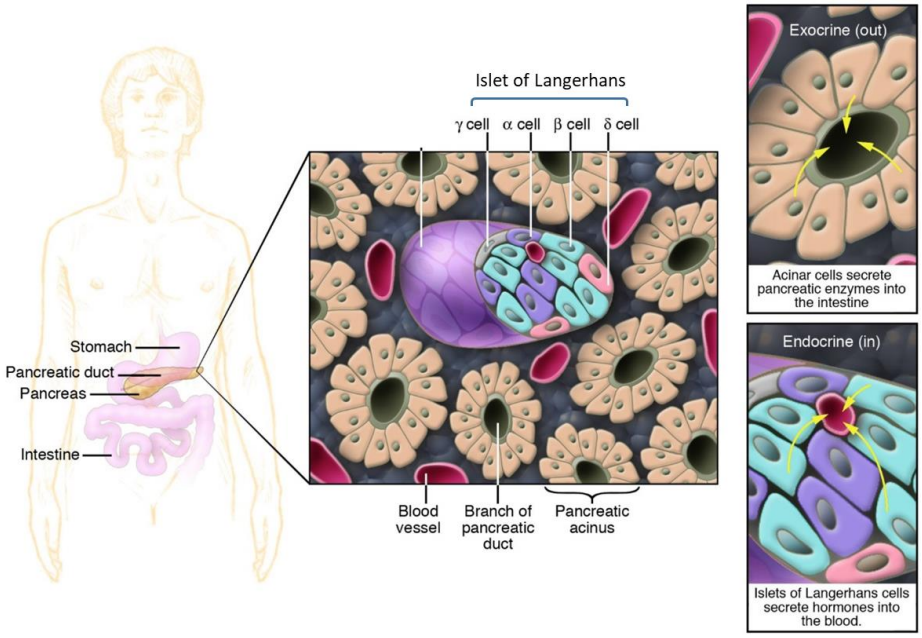

Figure 1. Cross section of the pancreas

Adapted from (15)

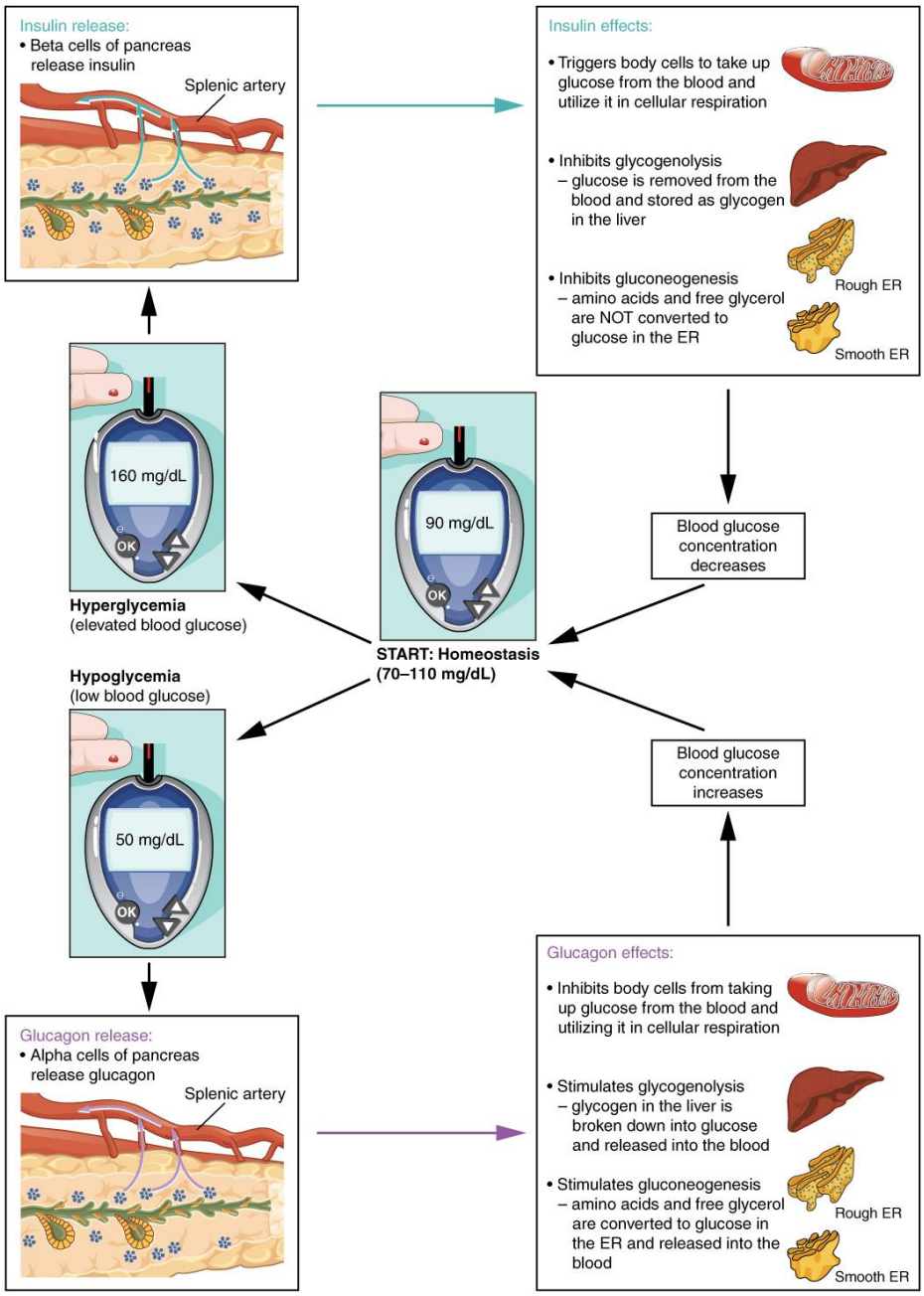

Figure 2. Homeostatic regulation of blood glucose level

Adapted from (6)

1.5.2.1. Insulin

Insulin is a key anabolic hormone that is secreted by pancreatic β-cells in response to high blood glucose level. Insulin brings glucose to tissues for respiration or to the liver where the glucose is stored as glycogen. By promoting glucose uptake by cells throughout your body for respiration and protein and fat synthesis while suppressing glucagon secretion or by signaling the body to store excess glucose in the liver, insulin lowers the concentration of glucose in the blood (19). The stored glycogen is not released until the blood glucose levels fall below the normal range (20). As insulin plays the main role in glucose homeostasis, making and releasing the right amount of insulin according to the blood glucose level and responding properly to insulin are important for the maintenance of glucose homeostasis (16). When there is too little insulin (termed hypoinsulinemia), it results in high blood glucose levels. Excess glucose spills into the urine, which leads to dehydration (21). In addition, the cells cannot use glucose for energy and make new energy from fat which makes acids as waste products. Eventually, this can lead to coma and death if one does not receive medical attention (22).

On the contrary, when there is too much insulin (termed hyperinsulinemia), this leads to abnormally low blood glucose levels, which is called hypoglycemia. If it is not treated promptly, it will affect the brain, which depends almost entirely on blood glucose as a source of energy. Ultimately, it can cause dizziness and even coma (23).

Producing the right amount of insulin is important, but responding properly to insulin is also significant factor for keeping the blood glucose level in a narrow range. When cells stop responding to insulin, the condition is called insulin resistance (24). Even though there is enough insulin available in the blood, our body is resistant to insulin or has low insulin sensitivity, both insulin and blood glucose levels rises. As this condition continues for a long time, the pancreas fails to keep up with the increasing blood glucose and may become damaged (25).

1.5.2.2. Glucagon

Glucagon is a key catabolic hormone secreted from pancreatic α-cells. It maintains plasma glucose during fasting conditions by promoting breakdown of store liver glycogen, a process called hepatic glucose production. It also promotes hepatic gluconeogenesis and hepatic ketogenesis and brings the dropped blood glucose back to the normal range (26).

1.5.2.3. Somatostatin

Somatostatin is secreted by pancreatic δ-cells upon glucose stimulation after food intake. It inhibits insulin and glucagon release from pancreatic islets to prolong the absorption of nutrients by the tissues. It prevents quick depletion of nutrients in the bloodstream (27).

1.5.2.4. Pancreatic polypeptide

Pancreatic polypeptides (PP) are secreted by pancreatic F cells. Its secretion is stimulated after exercise, fasting and acute hypoglycemia. It inhibits gallbladder contraction and secretion of pancreatic digestive enzymes (28).

2. Diabetes Mellitus

2.1. Overview

Glucose homeostasis is primarily maintained by pancreatic hormone, insulin, which enhances glucose storage or regulates glycogen breakdown, keeping the blood glucose level within a controlled range (29). When the β-cells produce insufficient amount of insulin or when the body cannot use the insulin properly, it leads to uncontrolled high blood glucose level or hyperglycemia, which is the hallmark of diabetes mellitus (30, 31). Diabetes mellitus is a group of metabolic disorders characterized by impaired glucose homeostasis resulting from impaired insulin secretion, insulin sensitivity, or both (32, 33). The number of people suffering from diabetes mellitus has been rising rapidly in the past three decades. In addition, diabetes mellitus is expected to be the seventh leading cause of death in 2030 worldwide (34, 35).

2.2. Symptoms

As the duration of diabetes gets longer, the chronic hyperglycemia of diabetes brings serious complications such as blindness, neuropathy, heart attacks, stroke and kidney failure (36). In addition, uncontrolled diabetes may also lead to stupor, coma, ketoacidosis or non-ketotic hyperosmolar syndrome which could result in death (32, 37).

2.3. Classification of Diabetes Mellitus

According to the classical classification of diabetes proposed by the American Diabetes Association (ADA), there are four different types of diabetes; type 1 diabetes (T1D), type 2 diabetes (T2D), gestational diabetes mellitus (GDM) and diabetes due to other causes such as cystic fibrosis, treatment of HIV/AIDS or after organ transplantation (38).

2.3.1. Type 1 Diabetes (T1D)

Type 1 Diabetes constitutes 5-10% of diabetes patients (39). It occurs due to autoimmune β-cell destruction, usually leading to absolute insulin deficiency and is more dominant in children and adolescents (32).

2.3.2. Type 2 Diabetes (T2D)

About 90-95% of diabetes patients belong to Type 2 Diabetes, which are observed mostly in adults (40). Progressive loss of β-cell

insulin secretion frequently on the background of insulin resistance develops hyperglycemia (41).

2.3.3. Gestational diabetes mellitus (GDM)

Gestational diabetes is diagnosed in the second or third trimester of pregnancy. Hyperglycemia in pregnancy is caused by not enough insulin production or related to the hormonal changes of pregnancy that make the body less able to use insulin (41).

2.3.4. Other types

Specific types of diabetes occurs due to other causes such as monogenic diabetes syndromes (e.g. neonatal diabetes and maturity-onset diabetes of the young), diseases of the exocrine pancreases (e.g. cystic fibrosis and pancreatitis), and drug- or chemical induced diabetes (e.g. treatment of HIV/AIDS or after organ transplantation) (41).

3. Mechanisms of Insulin Secretion

3.1. Overview

It is well known that upon elevation of blood glucose level, pancreatic β-cells secretes insulin, which is described as glucose-stimulated insulin secretion (GSIS) (42).

3.2. Electrical activity in pancreatic β-cells

Although pancreatic β-cells are not neuronal cells, insulin secretion in β-cells is associated with a complex electrical activity in the β-cells, which is characterized by a slow membrane depolarization along with bursts of action potentials (43). In fact, pancreatic β-cells share a large number of similarities with neuronal cells (44). Both cells express molecules such as glutamic acid decarboxylase (45), tyrosine hydroxylase (46), dopamine β-hydroxylase (47), type II voltage-dependent sodium channel (48), glutamate receptor (49), neurofilament proteins (50, 51), receptors for neurotrophins (52, 53), and thyrotropin-releasing hormone (54, 55). The resting membrane potential of β-cells is -60 ~ -70 mV with no electrical activities. The elevation of extracellular glucose gradually develops depolarization which activates voltage gated calcium channel (VGCC) in β-cells. Calcium influx through the VGCC triggers exocytosis of insulin granules (56).

3.3. K_{ATP}–channel dependent pathway

The primary pathway regulating the glucose-stimulated insulin secretion is through the activity of ATP-sensitive K^+ (K_{ATP}) channels (57). Extracellular glucose is transported into the β-cells by glucose transporter 2 (GLUT2) and metabolized by glycolysis which increases intracellular ATP/ADP ratio. The increased ATP level leads to closure of the K_{ATP} channel, which in turn evokes the depolarization of β-cells (58, 59) followed by the exocytosis of insulin granules from β-cells (56, 60,

61) as described in Figure 3.

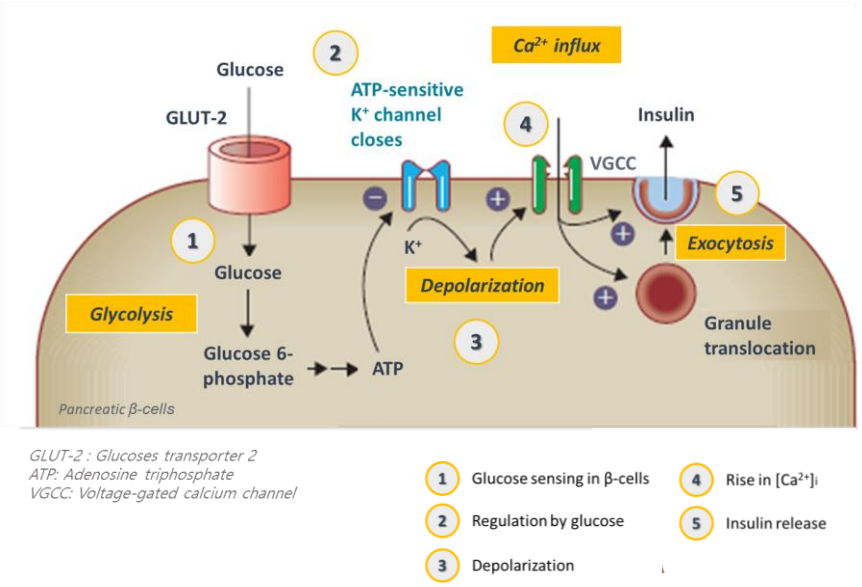

Figure 3. The mechanism of glucose-stimulated insulin secretion from the β-cells

Modified from (1)

3.4. K_{ATP}–channel independent pathway

Although the main triggering pathway for the glucose-stimulated insulin secretion is the K_{ATP}-dependent pathway, the involvement of K_{ATP} channel-independent pathways in the membrane depolarization induced by high glucose stimulation in β-cells has been also proposed (62-65). For example, electrical activity of β-cells is still triggered by glucose even when the K_{ATP} channel is non-functional (63) or in its gene-deleted mice (66-68).

3.4.1. Swelling-stimulated insulin secretion

As one of the candidate mechanisms for the K_{ATP} channel-independent insulin secreting pathways, β-cell swelling is considered in many studies (69-71). Without changes in extracellular glucose level, hypotonic stimulation still triggers insulin secretion in β-cells (62, 64, 72) Exposed to high concentration of glucose, metabolites, such as lactate, accumulate inside the β-cells that increases intracellular osmolality and induces water influx. Importance of metabolite accumulation is also proved in other study, as a non-metabolizable glucose analogue, 3-O-methylglucose, failed to evoke depolarization upon β-cell swelling (71, 73). Therefore, dependent on the glucose metabolism, high glucose induces swelling in β-cells and stimulates insulin secretion. As a mechanism underlying the swelling-stimulated insulin secretion, involvement of volume-regulated anion channels or stretch activated cation channels is proposed (Figure 4).

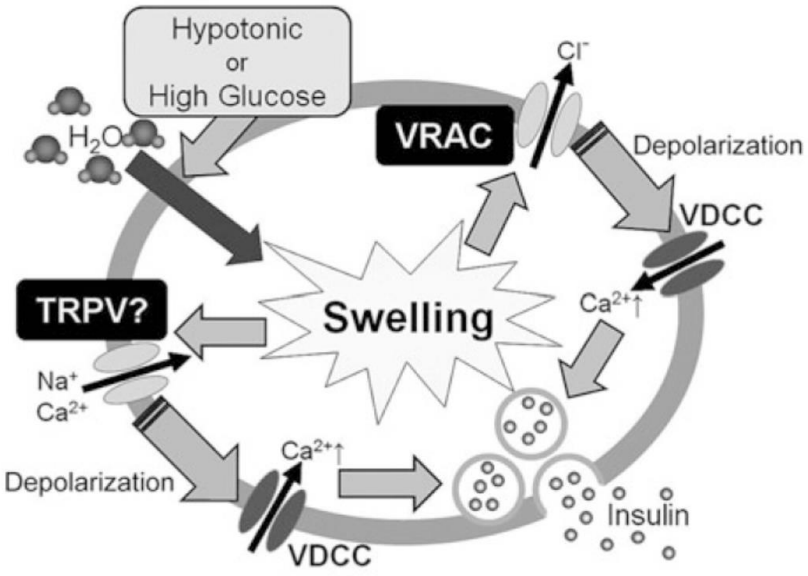

Figure 4. Mechanism of swelling-induced insulin secretion in β-cells

Adapted from (69)

4. Mechanotransduction

4.1. Overview

Mechanotransduction is referred to as the conversion of physical forces such as exercise, hemodynamic factors and osmotic change into biochemical signals (74). There are three steps required for the mechanotransduction: (1) the mechanical stimulus is sensed by the receptor cell; (2) the deformation ins transduced into an electrical signals; (3) the receptor potential is transmitted to the nervous system through action potentials (75).

4.2. Mechanically gated ion channels

Mechanically activated ion channels have pores in the plasma membrane, and mechanical stimuli increases their open probability (76). Upon mechanical stimulation, the passive diffusion of ions down their electrochemical gradient generates the membrane current (76). The best known mechanosensitive ion channels are potassium channels, TREK-1 and TRAAK, DEG/ENaC, TRP channels, TMC channels, and piezo channels (77). Recently one additional ion channel, TTN3, has been identified to be mechanosensitive (78).

4.3. Mechanosensitivity of pancreatic β-cells

Some of non-sensory cells and tissues derived from mesenchyme including endothelial cells are mechanosensitive. Pancreatic β-cells are derived from endodermal epithelium and are

known to be mechanosensitive (69). Indeed, mechanosensitive TRP channels are expressed in β-cells, and glucose stimulated insulin secretion is inhibited by mechanosensitive channel blockers (65). Cell swelling is well known indirect way of mechanical stimuli in pancreatic β-cells (69). Swelling leads to the stretch of the cell membrane, which in turn opens volume regulated or stretch-activated channels (71, 79).

4.3.1. Volume-regulated anion channels

Volume regulated anion channels is one of the promising candidates regulating the swelling stimulated insulin secretion pathway as it is activated by changes in cell volume (69). Several evidences showed that VRAC plays an important role in insulin secretion in β-cells: hypotonicity induced swelling of β-cells activated VRAC (62, 64); high glucose induced anionic currents resembling VRAC currents in β-cells (80, 81); and both glucose induced anionic currents and swelling-stimulated insulin secretion are blocked by a VRAC blocker, DCPIB (82). Recent studies found that SWELL1 (LRRC8A) mediates anion currents stimulated by high glucose induced swelling in mouse pancreatic β-cells (83, 84). Upon glucose-induced β-cell swelling, SWELL1 activation induced membrane depolarization and activation of VGCC-triggered calcium signaling, followed by insulin secretion. In addition, Swell1 KO mice show impaired glucose stimulated insulin secretion which is further exacerbated in mild obesity (83, 84).

4.3.2. Stretch-activated cation channels

Besides anion channels, the possible involvement of cation channels is also proposed in the swelling-stimulated insulin secretion, for several studies showed that glucose stimulated Ca^{2+} influx is not fully abolished with chloride blockers in K_{ATP} channel deficient β-cells (65, 85, 86). Indeed, its channel activity was observed as SAC channel blockers, such as gadolinium, amiloride, 2-APB, and ruthenium red, inhibit the swelling-stimulated insulin secretion in murine pancreatic β-cells (65, 69). Some transient receptor potential (TRP) channels, such as TRPV4 and TRPV2, have been proposed as candidate genes for SAC channels, however, there were no direct evidences that these TRP channels mediate the glucose-stimulated insulin secretion in β-cells (87, 88). Therefore, the molecular identity of SAC channel responsible for the glucose-induced cell swelling in pancreatic β-cells remains unknown.

5. Tentonin3

5.1. Overview

Our lab recently identified Tentonin 3 (TTN3/TMEM150C) as a cation channel activated by mechanical stimulation with unique slow inactivation kinetics (Figure 5) (78). TTN3 is a protein with 249 amino acids and have two paralogs, TTN1 and TTN2, with 26.5 % and 28.1 % similarity, respectively. It is also expressed in human (96 % similarity) and rat (99% similarity) (78).

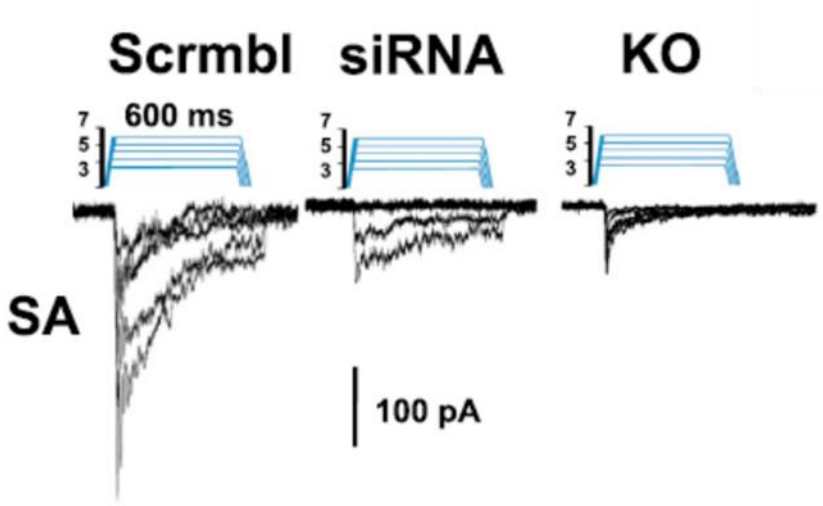

Figure 5. Slowly activating mechanosensitive currents evoked by TTN3

Adapted from (78)

5.2. Function

Mechanosensitive sensory input is essential in muscle coordination as the motor commands to one effector according to the sensory feedback from another effector (89). *Ttn3* KO mice showed less time clinging to an inverted grid and longer time to cross the beam. In addition, it showed an abnormal gait on the Catwalk automated gait analysis test. Hence, TTN3 regulates motor coordination by mediating mechanical transduction (78).

5.3. Expression profile

Tissue distribution assay using RT-PCR analysis shows that along with the dorsal-root ganglion neurons, TTN3 also expresses highly in mouse pancreas (78) (Figure 6).

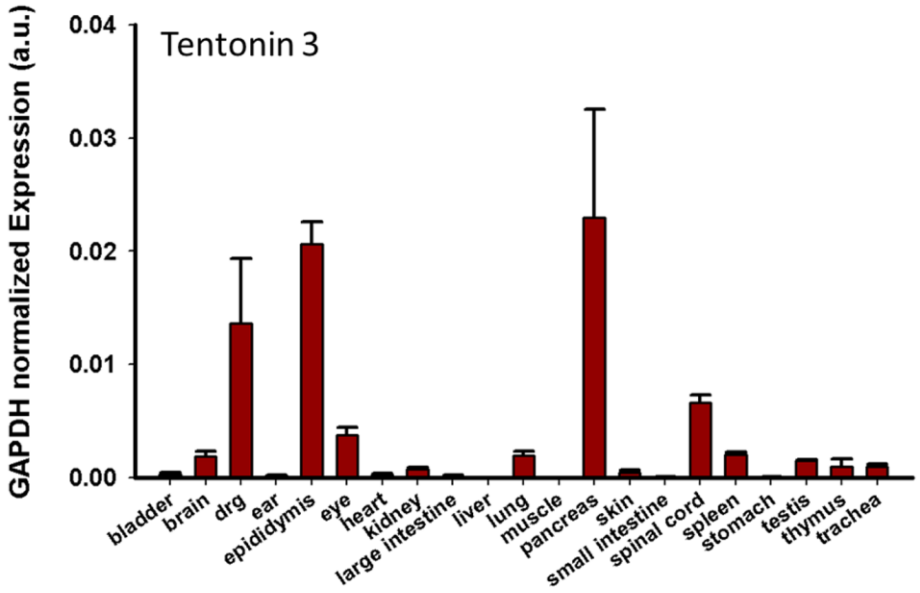

Figure 6. Expression profiles of TTN3 genes

Adapted from (78)

Purpose of the study

Glucose homeostasis maintains the blood glucose level within a narrow range by secreting two glucoregulatory hormones, glucagon and insulin from the pancreas. After having a meal. The pancreas secretes insulin which brings glucose to tissues for respiration. These bring the blood glucose level drop back to the normal range.

The primary pathway triggering the glucose-stimulated insulin secretion is through K_{ATP}-channel dependent pathway. But, the involvement of K_{ATP}–channel independent pathways have been also proposed. One of the candidates is high glucose-induced swelling stimulation. Swelling could activate two types of ion channels, volume regulated anion channel and stretch activated cation channel. Recently, the molecular identity of the anion channel was found that SWELL1/LRRC8A mediates anionic currents in response to β-cell swelling, however the molecular identity of the stretch activated cation channel remains unknown.

Previously, we confirmed that a novel mechanosensitive cation channel, TTN3, is highly expressed in pancreas (Figure 6). In the present study, we determined whether TTN3 mediates high glucose induced cationic currents in β-cells and contributes to the insulin secretion.

Methods

1. Animals

All animal experiments were conducted in accordance with protocols approved by the Institutional Animal Care and Use Committee (IACUC) at the Korea Institute of Science and Technology and ethical committee for animal welfare of the Seoul National University. TMEM150C knock out (KOMP, USA) male mice, ages 8-10 weeks, were used for experiments (78).

2. Immunohistochemistry

The pancreas tissue was fixed in formalin before embedding in paraffin, and cut in 5 μm serial sections. After deparaffinization with xylene and wash with serial dilutions of ethanol, sections were dehydrated followed by antigen retrieval. Primary antibodies used are; insulin (mouse monoclonal, sc-8033, 1:500), glucagon (mouse monoclonal, G2654,1:2000), amylase (mouse monoclonal, sc-46657, 1:500), mPiezo1 (rabbit polyclonal, NBP1-78537, 1:200), and TTN3 (rabbit polyclonal, manufactured, 1:200). Primary antibodies were detected by secondary antibodies conjugated to Alexa Flour 488 (A21202, 1:2000, Life Technology) and Alexa Flour 594 (A10072, 1:2000, Life Technology). Nucleus was stained using Hoechst 33342 (H3570, 1:5000, Thermo fisher Scientific). Images were captured using

a Zeiss LSM700 confocal laser scanning microscope (Carl Zeiss, Germany).

3. RNA interference

siRNA sequences were designed from the mouse TMEM150C sequence and synthesized by Bioneer (Korea). The sequences of three different siRNAs against TMEM150C used in calcium and insulin secretion assays were as follows:

(siRNA1) 5'-GCUUGUGGAUAGUGUACUU-3';
(siRNA2) 5'-CUUGUGGAUAGUGUACUUU-3';
(siRNA3) 5'-CAGAAGCUUCUGAAUAUCA-3'.

Negative control siRNAs provided by the manufacturer were used as control. Mixture of those three different siRNAs targeting TTN3 were transfected using RNAiMax (13778-030, Invitrogen) according to the manufacturer's protocol. RNA cells were processed and analyzed after 48 h of transfection.

4. RT-PCR

Total RNA was extracted using easy-spin TM Total RNA Extraction kit (17211, Intron, Korea) according to the manufacturer's instructions. Thereafter, cDNA was synthesized from 1 μg total RNA using SuperScript III (18080, Invitrogen, USA). RT-PCR was carried out

using DreamTaq Green DNA Polymerase (EP0712, Thermo Scientific, USA). Primers used for amplifying *Ttn3* were:

(Forward) 5'-GCGCTTCATCCAGCTAAAAC-3' and

(Reverse) 5'-AAGTACGCCAGGAAGCACAT-3'.

5. Primary culture of pancreatic β-cells

Mice were anesthetized using intraperitoneal injection of Zoletil (25 mg/kg) and Rumpon (10 mg/kg). Islets of Langerhans were isolated by injection of 4 ml HBSS containing 0.8 mg/ml collagenase P (11213865001, Roche, Germany) into the common bile duct. The pancreas was removed and incubated for 15 min in a water bath at 37°C. Islets were purified on Biocoll gradient (L6155, Biochrom, UK) and further isolated by two rounds of handpicking. Islets were cultured in RPMI 1640 medium (11875, Gibco, USA) supplemented with 10% FBS, penicillin (100 U/ml), and streptomycin (0.1 mg/ml) at 37°C and 5% CO_2. For patch clamp and calcium imaging, islets were dispersed into single cells by trypsin digestion.

6. Cell Culture

For cell culture studies, pancreatic β-cell lines, NIT-1, were cultured in RPMI 1640 medium (11875, Gibco, USA) supplemented with 10% FBS, 100 U/ml penicillin, and 0.1 mg/ml streptomycin. HEK293T cells were cultured in DMEM with 10% FBS, 100 U/ml penicillin, and 0.1

mg/ml streptomycin.

7. Calcium Measurements

NIT-1 cells, grown in 96-well plates, were incubated with Fluo-4 NW (F36206, Invitrogen, USA) for 1 h at 37°C and washed with isotonic (290 mOsm/kg) buffer solution. Fluo-4 NW was excited at 488 nm and emitted at 535 nm. The ratio of the fluorescence change, F/F0, was plotted to represent the changes in intracellular Ca^{2+} levels in response to 20 mM glucose or hypotonic (210 mOsm/kg) solution using SPARK 10M Multi reader (Tecan, Switzerland). Isolated pancreatic β-cells were loaded with Fura-2-AM (F1221, Molecular Probes, USA) HBSS buffer at 37°C for 30 min. The cells were perfused with isotonic (290 mOsm/kg) buffer solution and changed with either high glucose (20 mM) or hypotonic (210 mOsm/kg) solutions. Depolarization of the cells with 30 mM KCl was used as positive control at the end of the measurement. Fluorescent signals in single β-cells were imaged every 3 s via 340 nm excitation and 380 nm emission filters. All imaging data were collected by Meta Flour software (Molecular Devices, USA). The ratios of fluorescence were calculated and analyzed using a digital fluorescence analyzer (MetaFlour, Molecular Devices, USA) (90). For both measurements, isotonic (290 mOsm/kg) buffer solution contained (in mM): 85 NaCl, 5 KCl, 1.2 $MgCl_2$, 1.2 $CaCl_2$, 10 HEPES, 2.8 Glucose, and 100 D-mannitol (pH7.4). Hypotonic (210 mOsm/kg) buffer contained (in mM): 85 NaCl, 5 KCl, 1.2 $MgCl_2$, 1.2 $CaCl_2$, 10 HEPES, and 2.8

Glucose (pH7.4). High glucose (20 mM) buffer contained (in mM): 85 NaCl, 5 KCl, 1.2 $MgCl_2$, 1.2 $CaCl_2$, 10 HEPES, 2.8 Glucose, and 100 D-mannitol (pH7.4).

8. Electrophysiology

For recording currents in HEK293T or primary β-cells, intracellular potential (pipette voltage) was clamped at – 60 mV. Whole cells were formed after rupturing the membrane under a glass pipette. The tip resistance was 2-3 MΩ. The junctional potential was canceled to zero when the tip was immersed to the bath solution. Currents were amplified with an Axopatch 200B amplifier (Molecular devices, USA), filtered at 10 kHz (Low pass Bessel filter) and sampled at either 5 or 10 kHz (Digidata 1440A, Molecular Devices, USA). For current clamp recordings, bias current was not injected. Data were analyzed using programs written in MATLAB (MathWorks, USA). Resting membrane potentials were measured as averaged membrane potential for 10 s before applying high glucose or hypotonic stimulations. The number of action potentials, firing rates, peak voltage, and amplitude were measured as baseline subtracted averages during the firing activity of the cell.

9. Solutions

For recording current responses to mechanosensitivity in primary β-cells and hypotonicity in HEK293T cells, the basal extracellular

solution contained (in mM): 90 NaCl, 2 KCl, 1 $MgCl_2$, 1 $CaCl_2$, 10 HEPES, and 90 D-mannitol (pH7.2), while hypotonic solution contained the same components with the exemption of D-Mannitol. The pipette solution contained (in mM): 130 CsCl, 2 $MgCl_2$, 10 HEPES, 2 Mg-ATP, 0.2 Na-GTP and 30 D-mannitol (pH 7.2). To block Cl^- current, Na-gluconate solution was used; the isotonic (287 mOsm/kg) bath solution contained (in mM): 100 Na-Gluconate, 2 $CaCl_2$, 10 HEPES, 90 D-Mannitol (pH 7.21). Hypotonic solution contained the same components with the exemption of D-Mannitol. Osmolality was also adjusted with mannitol for 20mM glucose stimulation. The intracellular solution (287 mOsm/kg) contained (in mM): 100 Na-Gluconate, 10 HEPES, 90 D-Mannitol (pH 7.21). For current clamp recordings, the isotonic (280 mOsm/kg) bath solution consisted of (in mM): 85 NaCl, 5 KCl, 10 HEPES, 1.2 $MgCl_2$, 1.2 $CaCl_2$, and 90 D-mannitol (pH 7.3 with NaOH). For hypotonic (200 mOsm/kg), osmolarity was adjusted with D-mannitol. Glucose concentration for standard bath solution was either 0 mM or 2.8 mM, whereas high glucose stimulation was by 20 mM Glucose. The pipette solution contained (in mM): 138 KCl, 10 NaCl, 1 Mg Cl2, 10 HEPES, 10 EGTA (pH 7.3 with KOH), 5 ATP, and 0.1 GTP.

10. Mechanical Stimulation

Mechanical stimulations were carried out as described previously (78). Briefly, a fire-polished thin glass electrode (tip diameter 3–4 μm) was positioned at an angle of ~50° to the cell surface. Controlled by a

micromanipulator (Nano-controller NC4; Kleindiek Nanotechnik), the glass probe moved downward in a series of mechanical steps in 1 μm during the ramp segment of the command. The typical duration of the mechanical stimulation was 600 ms.

11. Glucose Tolerance Test

For glucose tolerance tests, mice were fasted for 16 h and then injected with D-Glucose (2 g/kg body weight). Blood samples were collected via the tail at 0, 15, 30, 45, 60, and 120 min after intraperitoneal glucose injection. Glucose levels were measured by OneTouch Ultra blood glucose meter (LifeScan, USA).

12. Insulin Tolerance Test

For insulin tolerance tests, mice were fasted for 6 h and then injected with Humulin R (0.5 U/kg). Blood samples were collected via the tail at 0, 15, 30, 60, and 120 min after intraperitoneal insulin injection. Glucose levels were measured by OneTouch Ultra blood glucose meter (LifeScan, USA).

13. Insulin Secretion Assay

NIT-1 cells were cultured in 6-well plates and washed twice with glucose-free HEPES-balanced Krebs-Ringer-Bicarbonate buffer (KRBH) and then pre-incubated with glucose-free Rosewell Park

Memorial Institute 1640 medium for 2 h at 37°C and in 5% CO_2. Cells were then pre-incubated in KRBH buffer for 1 h at 37°C and in 5% CO_2. After removal of the pre-incubation solution, the cells were incubated in KRBH buffer containing low (2.5 mM) glucose or high (16.7 mM) glucose solution for 1 h. Incubation media was collected, and the amount of insulin was measured using ELISA (ALPCO, Salem). The insulin level was adjusted for total cellular protein of cell lysate. The measurement from the plate of cells with the control medium stimulated by low glucose was considered as 100% of glucose-stimulated insulin secretion. For serum insulin measurement, blood samples were collected via the tail at 0, 10, 20 and 30 min after intraperitoneal glucose injection (2 g/kg body weight). After centrifugation at 2500 rpm, Ultra Sensitive Mouse Insulin ELISA Kit (90080, Crystal Chem, USA) was used to determine the serum insulin values.

14. Statistics

Data are presented as means **±** S.E.M. Comparisons between groups were performed by two tailed unpaired Student's *t* test. Multiple comparisons of the means were analyzed with one-way ANOVA with Tukey's post-hoc tests. P values less than 0.05 are considered significant.

Results

1. The expression of TTN3 in pancreatic β-cells

Previous finding revealed that TTN3 shows high mRNA expression level in mouse pancreas (78). To further analyze detailed localization pattern of TTN3 in pancreas, sections of mouse pancreas were stained with TTN3 antibody together with pancreatic cell markers. Surprisingly, pancreatic cells that are insulin-positive only expressed TTN3 (Figure 7), while an exocrine marker, amylase, or an alpha cell marker, glucagon, failed to colocalize with TTN3.

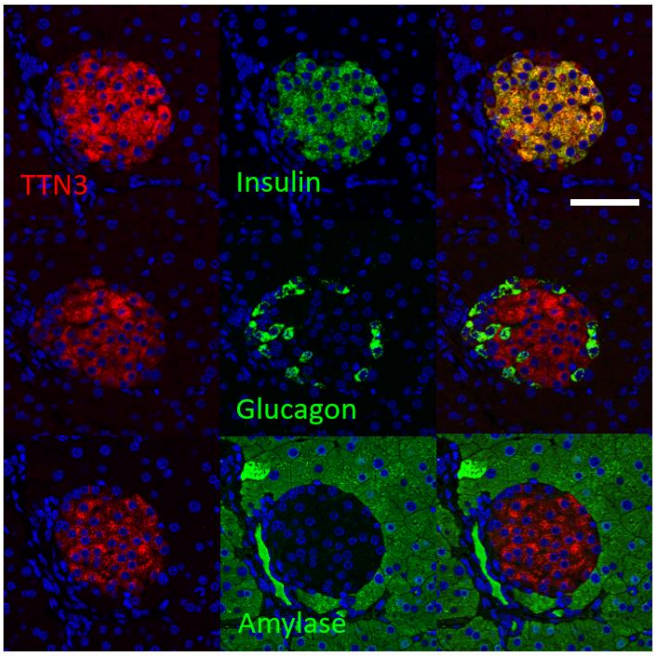

Figure 7. Immunofluorescence analysis of TTN3 in mouse pancreas

Immunofluorescence staining of TTN3 (red) and insulin (green, upper panels), glucagon (green, middle panels), or amylase (green, lower panels) in mouse pancreas sections. Scale bar represents 50 µm.

2. Primary cell culture of β-cells from *Ttn3* KO mouse

2.1. TTN3 systemic KO mouse

To analyze the role of a novel cation channel TTN3 in β-cells, we used TTN3 knockout (KO) mouse. Mouse was generated by the trans-National Institutes of Health Mouse Initiative Knockout Mouse Project. Insertion of LacZ sequence with stop codon between the exons 5 and 6 of the Ttn3 locus resulted in the constitutive KO (non-conditional) mouse model (Figure 8) (78) .

2.2. Islet morphology of WT and *Ttn3* KO mice

We analyzed the islet morphology of WT and *Ttn3* KO mice appeared grossly similar and normal (Figure 9), indicating that β-cell itself is intact from the loss of *Ttn3*.

2.3. Isolation of pancreatic islets

Pancreatic islets were isolated and purified using Biocoll gradients (Figure 10A). We conducted mRNA expression level in mouse β-cell line, NIT-1 cells, and pancreatic islets isolated from wild type (WT) mice and *Ttn3* KO mice. *Ttn3* transcripts were observed in NIT-1 cells and WT pancreatic islets, but not in *Ttn3* KO islets (Figure 10B).

2.4. Expression of TTN3 in mouse pancreatic islets and β-cell line

For the functional study of TTN3, isolated islets were further dissociated into single β-cells using trypsin, and β-cells were identified by their large size and granular morphology (91, 92). These dissociated cells clearly displayed TTN3 and insulin co-expression (Figure 11). In addition, α-cells are electrically active in the absence of glucose unlike β-cells as they express different types of voltage-gated Ca^{2+} channels (93, 94). So, identifying β-cells by their morphology and inactivation at low glucose is sufficient for further study of TTN3 in isolated pancreatic β-cells.

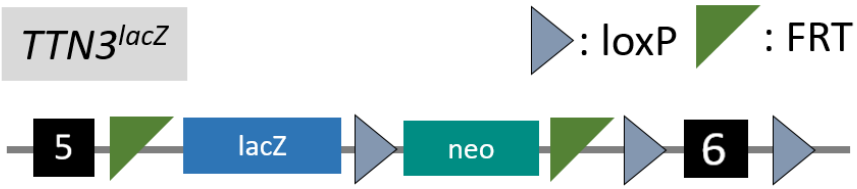

Figure 8. Schematic illustration of constitutive *Ttn3* KO mouse

Adapted from (78)

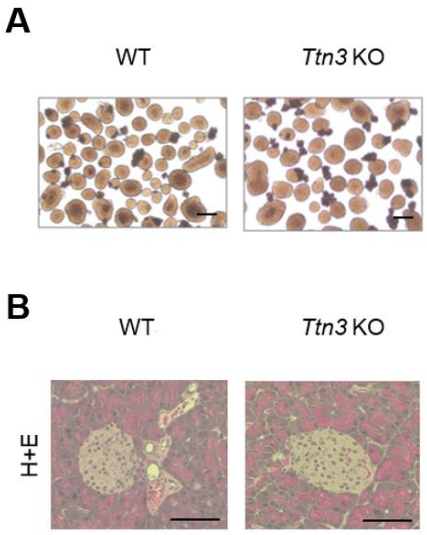

Figure 9. Islet morphology of *Ttn3* KO mice

(A) Representative photographs of freshly isolated pancreatic islets from WT (left) and *TTN3* KO mice (right). Scale bars: 200 µm.

(B) Pancreatic islets from WT and *Ttn3* KO mice stained with hematoxylin-eosin (H+E). Scale bars: 200 µm.

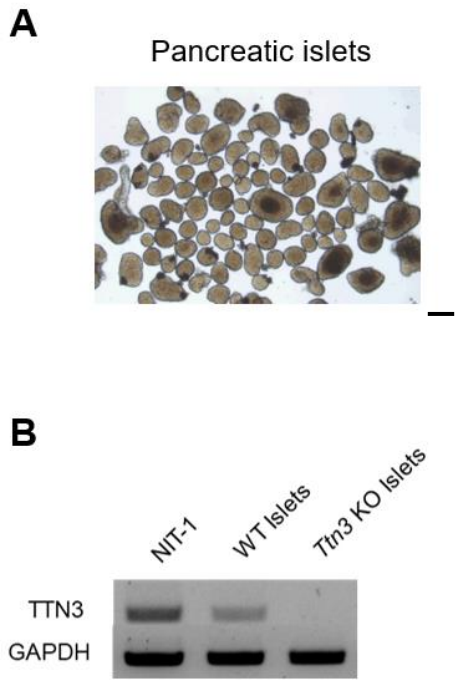

Figure 10. Isolation of mouse pancreatic islets

(A) Representative photographs of freshly isolated pancreatic islets from WT mice. Scale bars: 200 μm. Freshly isolated pancreatic islets are further incubated in trypsin and dispersed into single cells.

(B) RT-PCR analysis for gene expression of TTN3 in mouse pancreatic β-cell line, NIT-1, and pancreatic islets of WT and *Ttn3* KO mice. GAPDH was used as a control.

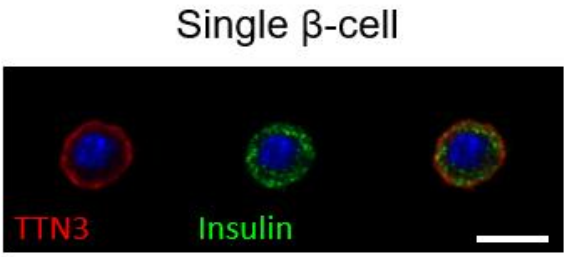

Figure 11. Immunofluorescence analysis of single pancreatic β-cell

Immunofluorescence staining of TTN3 (red) and insulin (green) in isolated pancreatic β-cell. Scale bar represents 10 μm.

3. TTN3 conducts mechanosensitive responses in mouse pancreatic β-cells

As TTN3 was initially identified as a mechanosensitive cation channel with distinct inactivation kinetics, we investigated if the slowly adapting currents to mechanical stimuli are observed in isolated β-cells. Using patch clamp technique, mechanical steps were applied on the isolated β-cells (Figure 12A). Indeed, the unique biophysical property of TTN3, the slowly adapting mechanically activated currents, were observed in WT β-cells (Figure 12B and D), but the currents were not observed in *Ttn3* KO β-cells (Figure 12C and D). These data indicate that TTN3 mediates mechanosensitive responses in mouse pancreatic β-cells.

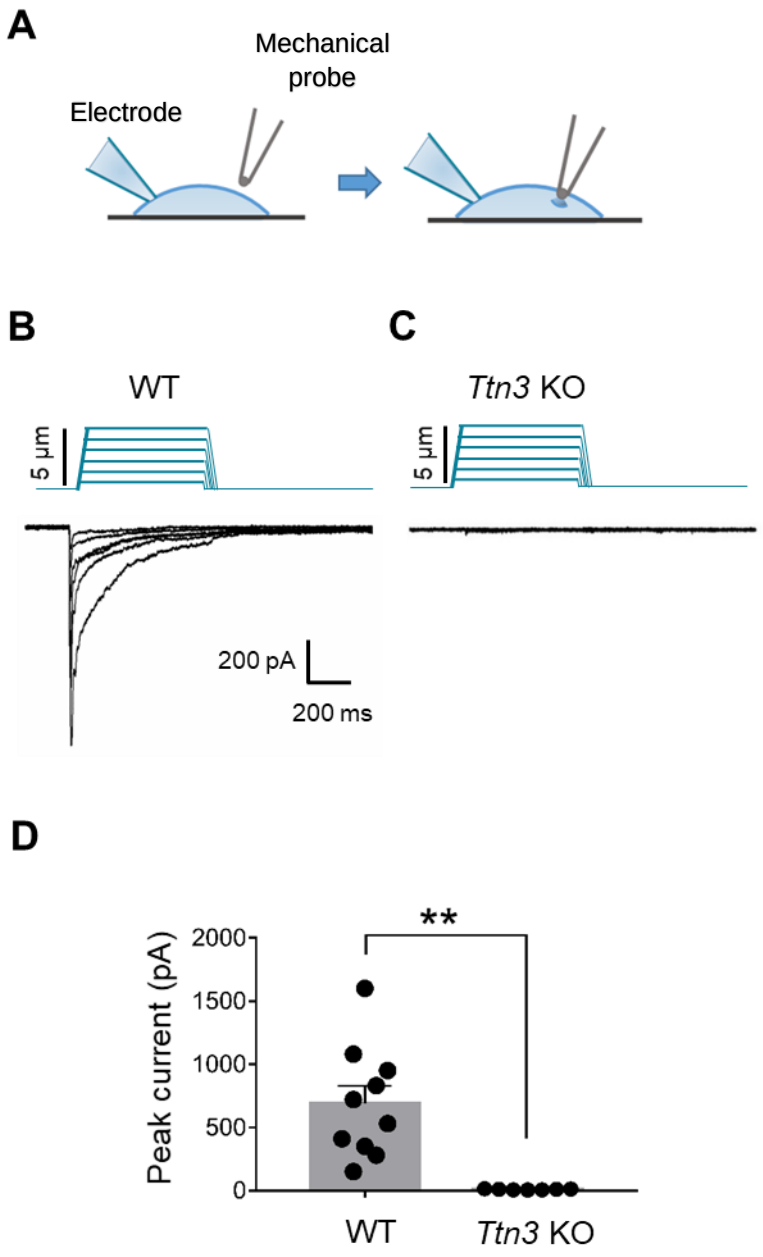

Figure 12. Mechanosensitive currents in β-cells

(A) The schematic diagram shows how mechanical stimulation is given to a cell during the patch clamp analysis.

(B-C) Representative traces of mechanically-activated inward currents elicited by different membrane displacement steps in primary β-cells from WT (A) and *Ttn3* KO (B) mice.

(D) Summary of peak amplitude of mechanically-activated currents measured in WT and *Ttn3* KO primary β-cells (n = 7-10). Data are presented as mean ± SEM. $^{**}p < 0.01$, Student's t test.

4. TTN3 is activated by hypotonicity-induced swelling

4.1. Overview

For cellular function, maintenance of a constant volume is essential against disturbances of body fluid osmolality (95). Upon external stimulations, acute cell swelling is occurred which is often followed by regulatory volume decrease (RVD). This restoration is achieved by activation of potassium and chloride conductance. Efflux of these ions followed passively by water is a key step in RVD (96). Volume regulated anion channels, playing a pivotal role in RVD, is ubiquitously expressed in mammalian cell (96, 97).

4.2. Activation of TTN3 by hypotonicity induced swelling in HEK 293T cells

In previous study on TTN3, its activation was studied only using a direct mechanical stimulation. Hypotonicity-induced cell swelling is an indirect way of mechanical stimuli (69). So, we next determined whether TTN3 is also activated by the indirect mechanical stimuli, swelling. We transfected *Ttn3* to human embryonic kidney 293T (HEK293T) cells and stimulated by hypotonic (200 mOsm/kg) solution. As HEK293T cells innately expressed endogenous VRAC channels that evoke large inward currents to hypotonic solution (Figure 13A). These currents were blocked by a chloride channel blocker, fluoxetine (100 μM) (98) (Figure

13B). In HEK293T cells transfected with *Ttn3*, however, the hypotonic solution induced robust inward currents even in the presence of 100 μM fluoxetine (Figure 13C). The current-voltage relationship was further determined to confirm that ionic flux observed in *Ttn3*-overexpressed HEK293T cells in the presence of fluoxetine is cationic currents (Figure 13D). TTN3 is activated by hypotonicity-induced cell swelling.

4.3 Activation of TTN3 by hypotonicity induced swelling in isolated pancreatic β-cells

We next explored the swelling mediated cationic currents by TTN3 in isolated pancreatic β-cells. To exclude the involvement of anionic currents in response to volume change, intracellular Cl^- was replaced with the impermeable anion, Na-gluconate (99) (Figure 14A). The application of hypotonic (200 mOsm/kg) solution robustly evoked inward currents in isolated β-cells of WT mice, while the currents were markedly reduced in *Ttn3* KO β-cells (Figure 14B-D).

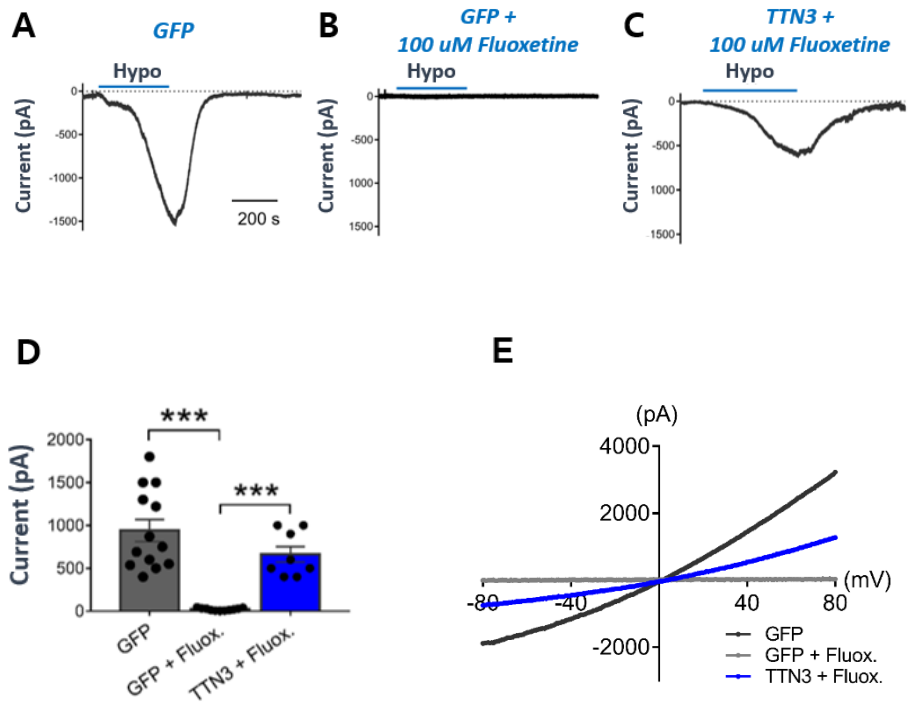

Figure 13. TTN3 activation by swelling in HEK293T cells

(A-B) Representative trace of hypotonicity (210 mOsm/kg)-induced currents in HEK293T cells transfected with *Gfp* in control bath solution (**A**) and in the presence of 100 μM fluoxetine, a volume-regulated anion channel blocker (**B**). Note a complete block of volume-regulated anion channel current by fluoxetine.

(C) Representative traces of hypotonicity (210 mOsm/kg)-induced currents in HEK293T cells transfected with *Ttn3* in the presence of 100 μM fluoxetine. Note a robust current evoked by the hypotonicity in the presence of fluoxetine.

(D) Summary of amplitudes of hypotonicity-induced currents in HEK293T cells transfected with *Gfp* or *Ttn3* in the absence or presence

of fluoxetine (n = 8-13). *** $p < 0.001$, one-way ANOVA with Tukey's *post-hoc* test.

(E) Representative current-voltage (I-V) relationships of hypotonicity-induced currents in HEK293T cells expressing *Gfp* or *Ttn3* in the absence (dark grey) or presence of fluoxetine.

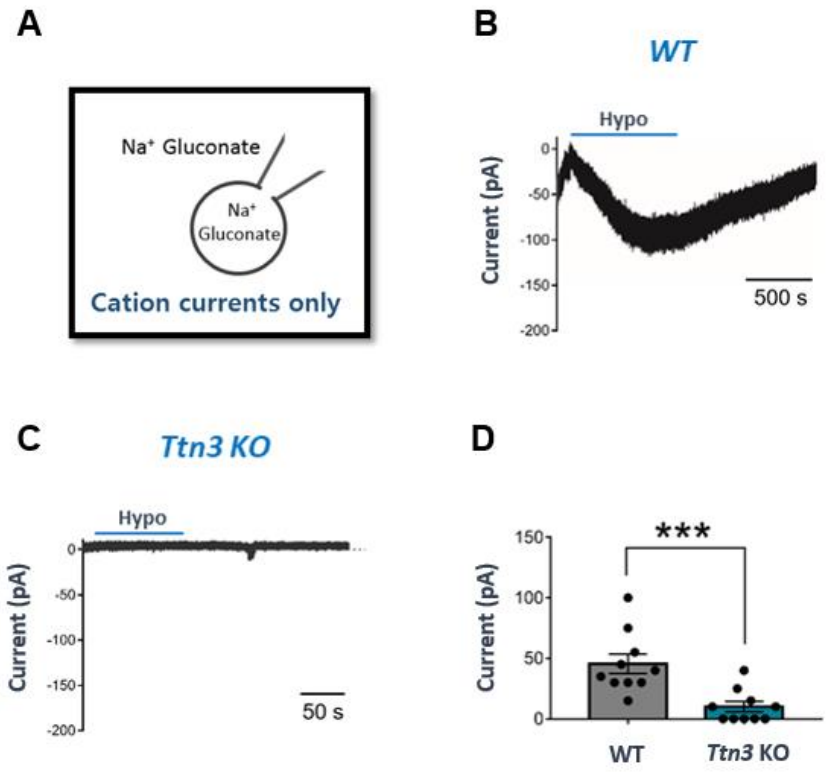

Figure 14. TTN3 activation by swelling in pancreatic β-cells

(A) In order to block anion currents, both the pipette and bath solutions contained sodium gluconate as main charge carriers.

(B-C) Representative traces of hypotonicity (210 mOsm/kg)-induced currents in primary β-cells from WT (**B**) and *Ttn3* KO (**C**) mice.

(D) Summary of amplitude of the hypotonicity-induced currents in WT and *Ttn3* KO primary β-cells (n = 10 / genotype). *** $p < 0.001$, Student's t test.

5. TTN3 is activated by high glucose-induced swelling

We next determined whether glucose-induced swelling is also sufficient to evoke currents through TTN3 in β-cells, as high glucose results in β-cell membrane stretch due to the osmolality changes derived by the accumulation of metabolites (69-71). Similar to the hypotonic stimulation, the application of high glucose (20 mM) also evoked inward currents in WT pancreatic β-cells, but the responses were significantly reduced in *Ttn3* deficient β-cells (Figure 15A-C). These data suggest that TTN3 mediates cationic currents upon high glucose-induced swelling in mouse pancreatic β-cells.

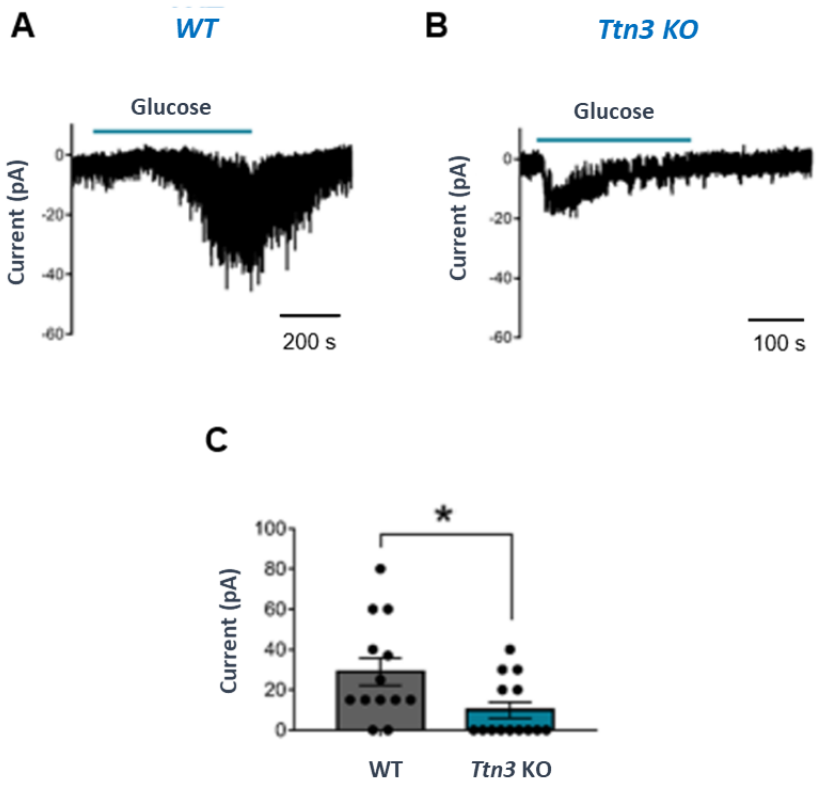

Figure 15. TTN3 activation by glucose in pancreatic β-cells

(A-B) Representative traces of high glucose (20 mM)-induced currents in β cells from WT (**A**) and *Ttn3* KO mice (**B**). Both the pipette and bath solutions contained sodium gluconate as main charge carriers.

(C) Summary of amplitude of glucose-induced inward currents in WT and *Ttn3* KO primary β-cells (n = 14 / genotype). * $p < 0.05$, Student's t test.

6. TTN3 activation contributes to the glucose-evoked depolarization of β-cells

Pancreatic β-cells are excitable cells eliciting action potential firings in response to glucose stimulation (100, 101). In order for β cells to secrete insulin, the cells need to be depolarized first. The electrical activity is initiated by ion fluxes throughout the β cells, such as Ca^{2+}, Na^{+} (102) and Cl^{-} (103). As shown in Figure 15, the loss off TTN3 reduced high glucose mediated cationic currents in β cells, we thus asked whether ablation of TTN3 could also contribute to the action potentials in β cells. Therefore, we determined if TTN3 contributes to the glucose-induced electrical activities of β-cells. Application of 20 mM glucose to isolated β-cells induced barrage of action potential firings along with depolarization (Figure 16A and Figure 17). However, glucose-induced spiking rates and membrane depolarization in *Ttn3* KO β-cells decreased significantly compared to those of WT β-cells (Figure 16B and Figure 17).

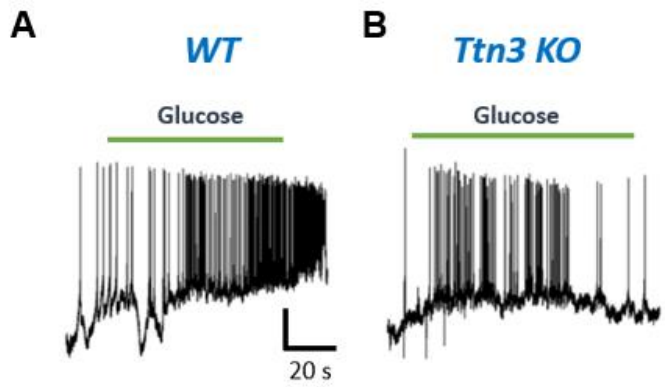

Figure 16. Electrical activities to glucose stimulation in β-cells

(A-B) Representative traces of high glucose (20 mM)-evoked electrical activity in WT (**A**) and *Ttn3* KO (**B**) primary β-cells.

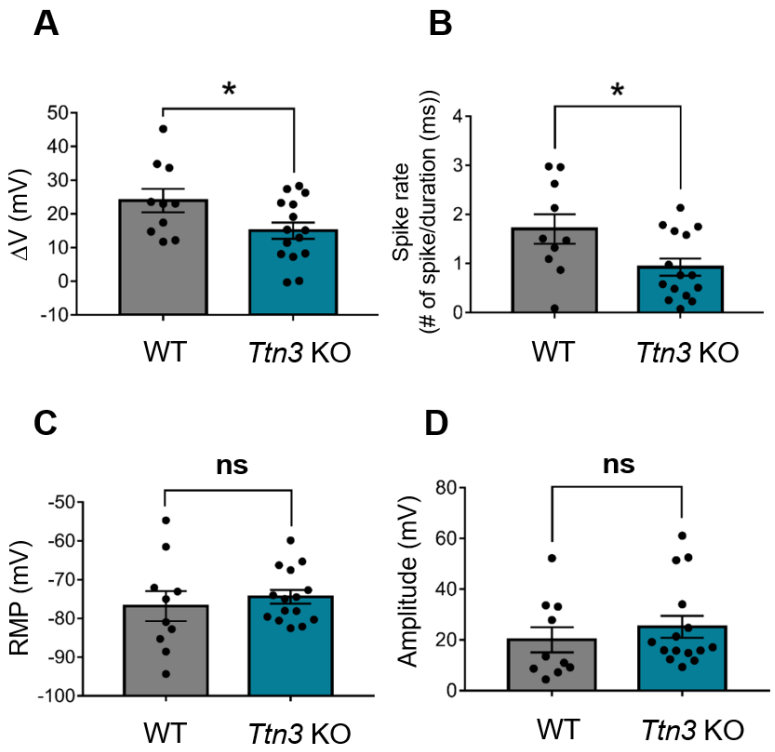

Figure 17. Analysis of electrical activities to glucose stimulation

(A-D) Summary of membrane depolarization (**A**), action potential firing rates (**B**), resting membrane potentials (RMP) (**C**), and amplitude of the firing activities (**D**) observed in WT and *Ttn3* KO primary β-cells in response to high glucose (20 mM) stimulation (n = 10-15). * $p < 0.05$, Student's t test

7. TTN3 activation contributes to the swelling-evoked depolarization in β-cells

We also determined contribution of TTN3 in swelling-stimulated depolarization in β-cells. Similarly, hypotonic (200 mOsm/kg) stimulation of β-cells from both genotypes evoked depolarization with action potential firings. In contrast, β-cells from *Ttn3* KO mice showed significantly reduced firing rates as well as depolarization (Figure 18 and Figure 19). The resting membrane potentials and amplitude of the firings of WT and *Ttn3* KO β-cells in response to both glucose- and hypotonic-stimulations were comparable (Figure 19). These results suggest that TTN3 is responsible for the electrical activity induced by glucose stimulation in β-cells.

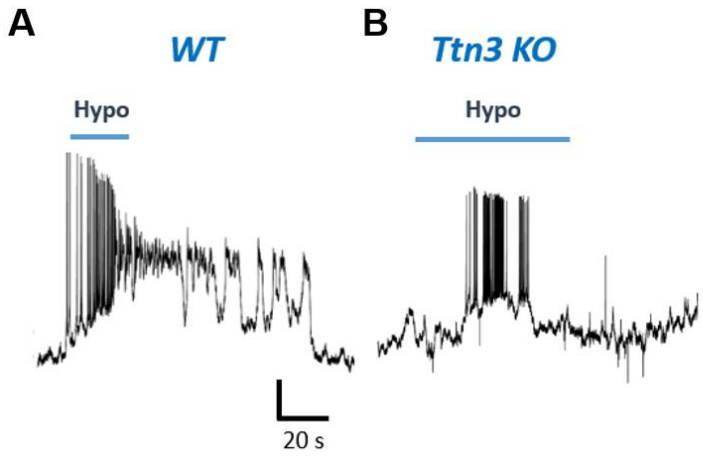

Figure 18. Electrical activities to hypotonic stimulation in β-cells

(A-B) Representative traces of hypotonicity (210 mOsm/kg)-evoked electrical activity in WT (**A**) and *Ttn3* KO (**B**) primary β-cells.

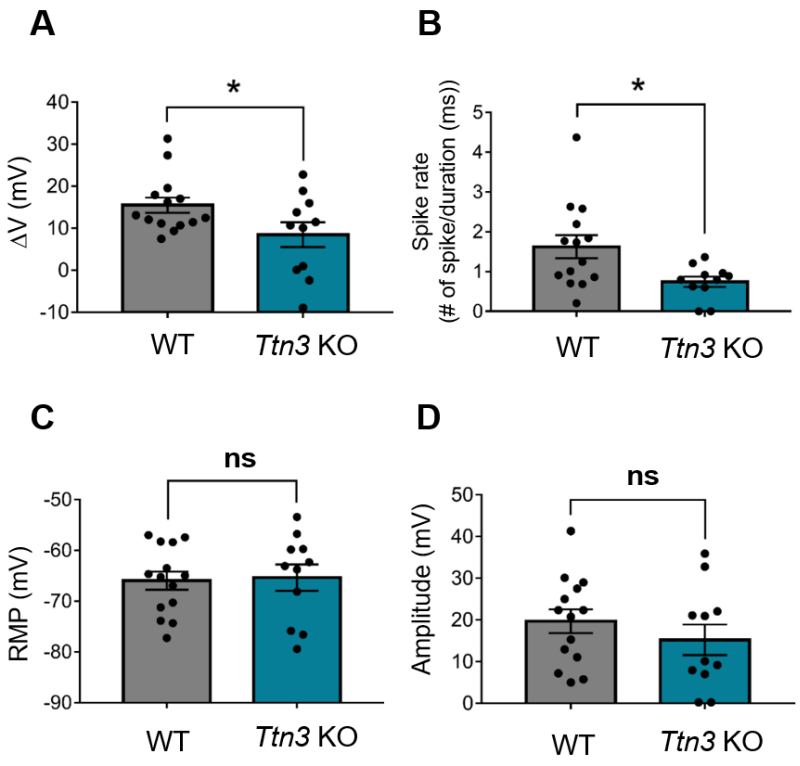

Figure 19. Analysis of electrical activities to hypotonic stimulation

(A-D) Summary of membrane depolarization (**A**), action potential firing rates (**B**), resting membrane potentials (RMP) (**C**), and amplitude of the firing activities (**D**) observed in WT and *Ttn3* KO primary β-cells in response to hypotonic (210 mOsm/kg) stimulation (n = 10-15). * $p < 0.05$, Student's t test.

8. TTN3 evokes Ca^{2+} influx to glucose stimulation

8.1. Calcium and Exocytosis

Subsequent to membrane depolarization, insulin secretion involves membrane docking, tethering and fusion of insulin granules. Insulin granules are defined into two groups depending on the site they are located. Those granules, pre-docked at the membrane and has interaction with SNARE and Ca^{2+}-regulated proteins, are called a readily releasable pool and the other granules, triggered only for the prolonged stimulation, are defined as a reserve pool (104, 105). For insulin granules to be secreted from the plasma membrane of β-cells, release from the fusion regulatory protein repressor, complexin, is required. Binding of Ca^{2+} to synaptotagmin, a Ca^{2+} sensor in the membrane of the pre-synaptic axon terminal, inhibits complexin and proceeds granules fusion and insulin secretion (106, 107). Consequently elevation of intracellular concentration of Ca^{2+} ($[Ca^{2+}]_i$) is significant mediator of GSIS in pancreatic β-cells (61).

8.2. TTN3-mediated Ca^{2+} influx in β-cell line, NIT-1

We determined the intracellular Ca^{2+} concentration, $[Ca^{2+}]_i$, of pancreatic β-cells to glucose- and hypotonic-stimulations. The application of high glucose (20 mM) solution elevated $[Ca^{2+}]_i$ rapidly in NIT-1 cells treated with scrambled small interfering RNA (siRNA). In contrast, the glucose-induced increase in $[Ca^{2+}]_i$ in N1T-1 cells transfected with *Ttn3* siRNA was significantly reduced (Figure 20).

Likewise, the hypotonic solution (210 mOsm/kg) caused a rapid elevation in $[Ca^{2+}]_i$ in scrambled siRNA-transfected NIT-1 cells, whereas *Ttn3*-siRNA transfected NIT-1 cells showed a significant decrease in the Ca^{2+} influx (Figure 21). The knock down of TTN3 was confirmed by RT-PCR (Figure 22).

8.3. TTN3-mediated Ca^{2+} influx to glucose stimulation in β-cells

Effects of TTN3 in the influx of Ca^{2+} to glucose stimulation in β-cells was observed. Similar to the β-cell line, NIT-1, glucose stimulation also evoked a sustained increase in $[Ca^{2+}]_i$ in WT β-cells whereas *Ttn3* KO primary β-cells showed significantly reduced Ca^{2+} responses (Figure 23). KCl (30 mM)-induced increase in $[Ca^{2+}]_i$ demonstrated that the β-cells are electrically viable in both genotypes (Figure 23). Together, these data demonstrate that TTN3 mediates glucose- and hypotonicity-induced Ca^{2+} influx in pancreatic β-cells. TTN3 mediates glucose-induced Ca^{2+} influx in pancreatic β-cells.

8.4. TTN3-mediated Ca^{2+} influx to hypotonic stimulation in β-cells

We next measured the changes in $[Ca^{2+}]_i$ of pancreatic β-cells to hypotonic stimulation. Hypotonic stimulation evoked a rise in $[Ca^{2+}]_i$ in WT β-cells. In contrast, the degree of increase in $[Ca^{2+}]_i$ was reduced in *Ttn3* KO primary β-cells (Figure 24). Treatment of high (30 mM) KCl

solution confirmed its electrical viability (Figure 24). TTN3 mediates hypotonicity-induced Ca^{2+} influx in pancreatic β-cells.

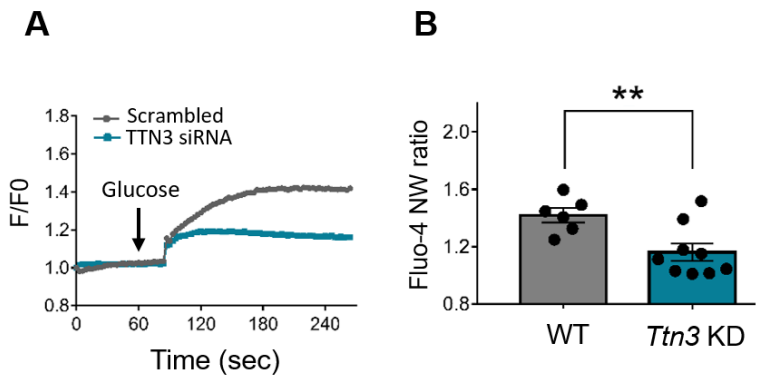

Figure 20. Glucose-stimulated Ca^{2+} influx in NIT-1 cells

(A) Average traces of intracellular Ca^{2+} to high glucose (20 mM) stimulation in Fluo-4 NW loaded mouse pancreatic β-cell line, NIT-1 cells, transfected with scrambled (grey) or *Ttn3* siRNA (cyan).

(B) Mean peak values of Fluo-4 NW fluorescence ratio in WT (grey) and *Ttn3* knock-down NIT-1 cells (cyan) to glucose stimulation (n = 6-9 wells). ** $p < 0.01$, Student's t test.

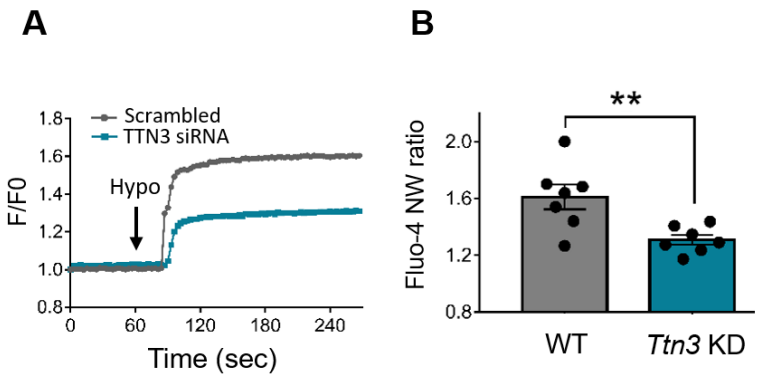

Figure 21. Swelling-stimulated Ca^{2+} influx in NIT-1 cells

(A) Average traces of intracellular Ca^{2+} to hypotonic (210 mOsm/kg) stimulation in Fluo-4 NW loaded mouse pancreatic β-cell line, NIT-1 cells, transfected with scrambled (grey) or *Ttn3* siRNA (cyan).

(B) Mean peak values of Fluo-4 NW fluorescence ratio in WT (grey) and *Ttn3* knock-down NIT-1 cells (cyan) to hypotonic stimulation (n = 7 wells / genotype). ** $p < 0.01$, Student's t test.

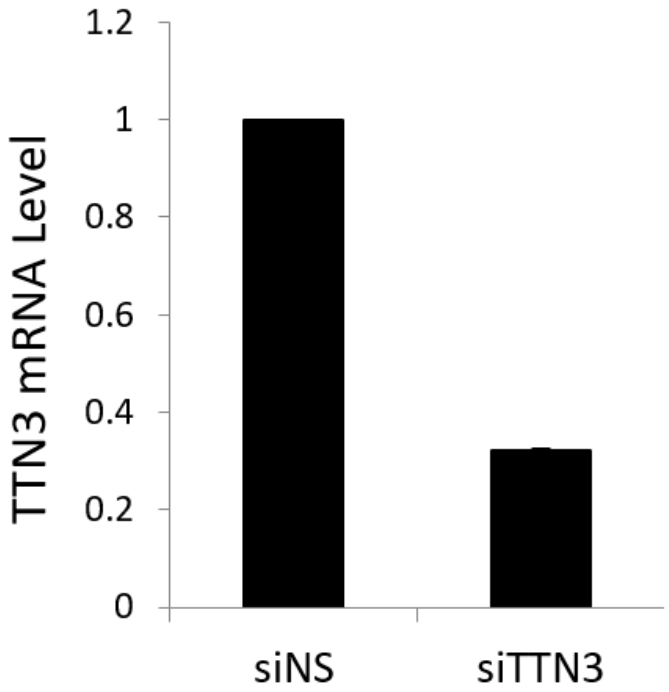

Figure 22. Knockdown of TTN3 in β-cell line, NIT-1

Treatment of siRNA targeting TTN3 decreased mRNA level of TTN3 in NIT-1 cells, mouse pancreatic β-cell line (*n* = 5).

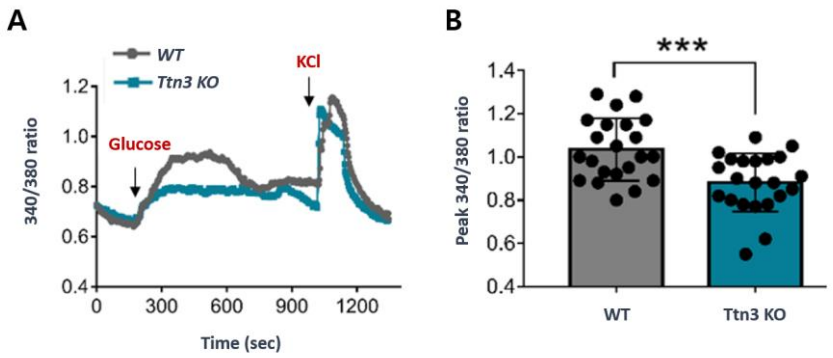

Figure 23. Glucose-stimulated Ca^{2+} influx in pancreatic β-cells

(A) Average traces of intracellular Ca^{2+} of Fura-2 loaded primary β-cells from WT (grey) and *Ttn3* KO mice (cyan) to high glucose (20 mM) stimulation. High KCl (30 mM) solution (arrow) was challenged to confirm cellular excitability.

(B) Mean peak values of the Fura-2 ratio (340/380 nm) from isolated WT (grey) and *Ttn3* KO (cyan) primary β-cells to high glucose stimulation. Fluorescence intensity was measured every 3 s (n = 22 / genotype). *** $p < 0.001$, Student's t test.

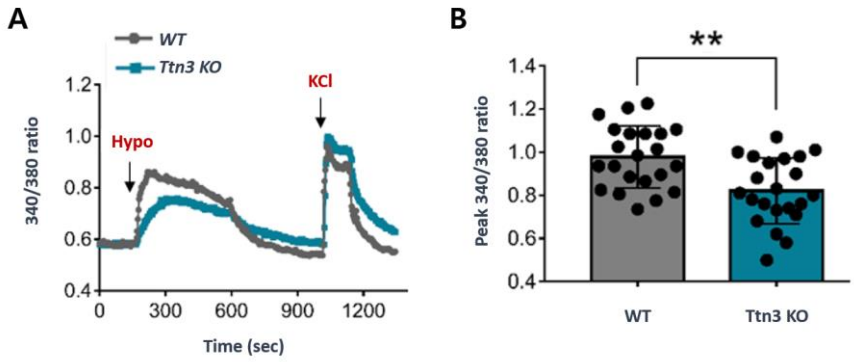

Figure 24. Swelling-stimulated Ca^{2+} influx in pancreatic β-cells

(A) Average traces of intracellular Ca^{2+} of Fura-2 loaded primary β-cells from WT (grey) and *Ttn3* KO mice (cyan) to hypotonic (210 mOsm/kg) stimulation. High KCl (30 mM) solution (arrow) was challenged to confirm cellular excitability.

(B) Mean peak values of the Fura-2 ratio (340/380 nm) from isolated WT (grey) and *Ttn3* KO (cyan) primary β-cells to hypotonic stimulation. Fluorescence intensity was measured every 3 s (n = 22 / genotype). ** $p < 0.01$, Student's t test.

9. TTN3-mediated Ca^{2+} influx and other pathways

9.1. K_{ATP} channel-mediated Ca^{2+} influx

The depolarization evoked by the closure of the K_{ATP} channel largely accounts for the increase in glucose-induced $[Ca^{2+}]_I$ (108). Therefore, to exclude K_{ATP} channel-derived Ca^{2+} influx in response to glucose stimulation, we treated an opener of K_{ATP} channel, diazoxide (109). In the presence of 100 μM diazoxide, WT pancreatic β-cells displayed a small but robust elevation of $[Ca^{2+}]_i$ in response to high glucose (20 mM). Surprisingly, the small elevation of $[Ca^{2+}]_i$ was reduced in *Ttn3* KO β-cells (Figure 25).

9.2. VRAC channel

In addition, swelling-stimulated $[Ca^{2+}]_I$ can also derived by two types of channels, stretch activated cation channel and VRAC. To determine whether TTN3-mediated $[Ca^{2+}]_I$ is related to the VRAC channel pathway, we blocked VRAC channel by fluoxetine (100 uM). The result showed that hypotonic stimulation still evoked a rapid and sustained increase in $[Ca^{2+}]_i$ in WT primary β-cells, whereas in *Ttn3* KO primary β-cells, the increase in $[Ca^{2+}]_i$ was reduced (Figure 26).

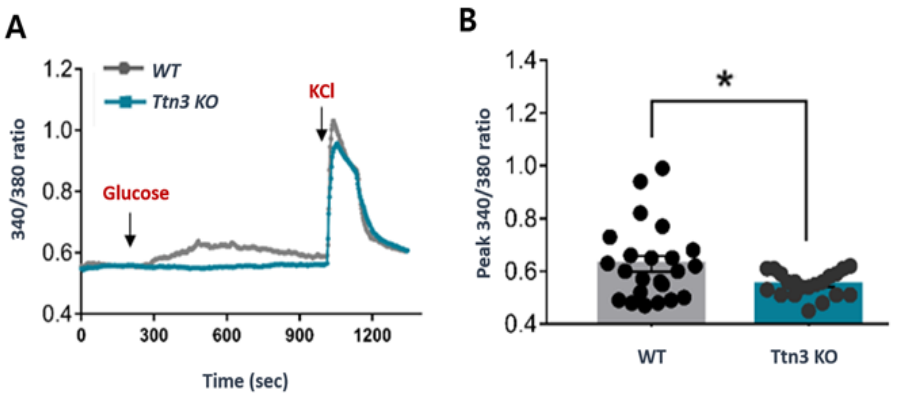

Figure 25. TTN3 mediates Ca^{2+} influx, independent of K_{ATP}-channel in response to glucose stimulation

(A) High glucose (20 mM)-induced intracellular Ca^{2+} of Fura-2 loaded primary β-cells from WT and *Ttn3* KO mice in the presence of K_{ATP} channel opener, diazoxide (100 μM).

(B) Mean peak values of Ca^{2+} transients of primary β-cells from WT and *Ttn3* KO mice in the presence of diazoxide (*n* = 20-23). * $p < 0.05$, Student's *t* test.

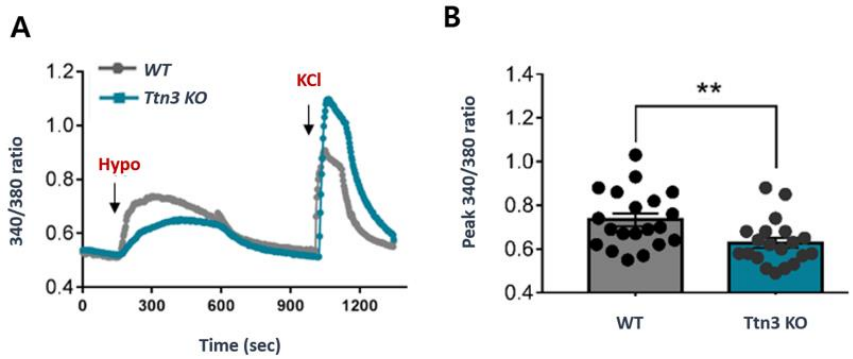

Figure 26. TTN3 mediates Ca^{2+} influx, independent of VRAC-channel in response to hypotonic stimulation

(A) Hypotonicity (210 mOsm/kg)-induced intracellular Ca^{2+} in Fura-2 loaded primary β-cells from WT and *Ttn3* KO mice in the presence of volume-regulated anion channel blocker, fluoxetine (100 µM).

(B) Mean peak values of Ca^{2+} transients of primary β-cells from WT and *Ttn3* KO mice in the presence of fluoxetine (*n* = 20 / genotype). ** $p < 0.01$, Student's *t* test.

10. Impaired glucose tolerance and insulin secretion in *Ttn3* KO mice

10.1. TTN3-mediated insulin secretion in NIT-1 cells.

Based on previous findings that the loss of TTN3 decreases Ca^{2+} influx and electrical activity of β-cells upon high glucose and hypotonic solutions, we next asked whether decreased Ca^{2+} influx in *TTN3* KO β-cells eventually leads to a reduction in insulin secretion and glucose tolerance. The amount of insulin released upon glucose stimulation was measured in NIT-1, treated with the scrambled siRNA or *Ttn3* siRNA. The application of high glucose (16.7 mM) solution to NIT-1 cells treated with scrambled siRNA induced 2.5-fold increase in insulin secretion compared to that of low glucose (2.5 mM) application. In contrast, the application of high glucose solution to NIT-1 cells transfected with *Ttn3* siRNA induced 1.6-fold increase in insulin secretion compared to that of the low glucose application to these cells (Figure 27).

10.2. *Ttn3* KO mice show higher blood glucose level upon glucose stimulation.

To determine the physiological role of TTN3 in glucose-stimulated insulin secretion, we assessed effects of *Ttn3* ablation on the ability to metabolize glucose. Next, the intraperitoneal (i.p.) glucose tolerance test was conducted in WT and *Ttn3* KO mice that were fasted overnight (16 h). I.p. injection of glucose (2 g/kg body weight) elevated

the blood glucose level in both genotypes. The basal blood glucose levels of both genotypes were comparable, however, *Ttn3* KO mice showed the significantly impaired glucose tolerance at 15min after the injection (Figure 28).

10.3. Insulin sensitivity is preserved in *Ttn3* KO mice.

As the ablation of *Ttn3* leads to the impaired glucose tolerance, we questioned whether the impaired glucose tolerance is due to decreased insulin sensitivity. Thus, we conducted i.p. insulin tolerance test (IPITT), where the serum glucose levels at different time points are measured before and after the injection of insulin (0.5 U/kg) in fasted (6 h) mice. As shown in Figure 29, blood glucose levels from both genotypes for two hours after the i.p. injection of insulin in fasted mice were identical, indicating that the loss of *Ttn3* does not alter the insulin sensitivity.

10.4. Decreased insulin secretion in *Ttn3* KO mice.

We next determined the effects of TTN3 on the glucose-stimulated insulin release *in vivo*. Serum insulin levels in every 10 min for the first 30 min after injection of glucose (2 g/kg body weight) in fasted (16 h) mice were measured. As shown in Figure 30, the injection of glucose elevated the serum insulin level in both genotypes in 10 min after the glucose stimulation. However, the serum insulin level in *Ttn3* deficient mice was significantly lower than that of WT mice. These

results suggest that the genetic ablation of *Ttn3* leads to impaired glucose tolerance due to the decreased insulin secretion.

10.5. Role of TTN3 in Diabetic disease models.

Next, we examined the effects of genetic ablation of TTN3 in mouse diabetic disease models. HFD feeding is used to induce mild obesity, a state of pre-diabetes (110). We induced diabetes by high fat feeding (HFD; 60% fat) for 12 weeks in mice and observed metabolic characteristics. Both genotypes gradually increased their body weight upon high fat diet, but *Ttn3* KO mice gained weight at faster rate and were significantly heavier compared to WT mice (Figure 31) with no differences in the amounts of water intake and food intake (Figure 32). Further studies are needed to determine what causes weight gain in *Ttn3* KO mice and the severity of glucose intolerance.

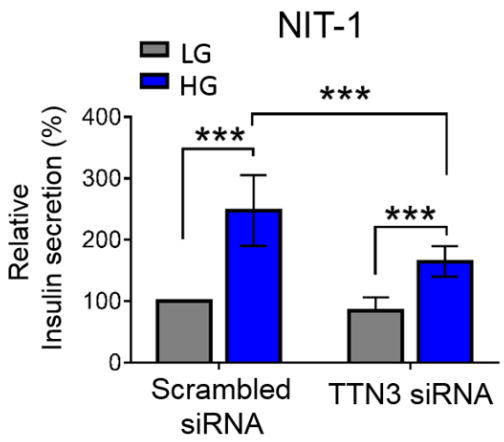

Figure 27. Measurement of insulin secretion in NIT-1 cells

Glucose-stimulated insulin secretion of NIT-1 cells treated with *Ttn3* siRNAs or scrambled siRNA to low glucose (LG, 2 mM) and high glucose (HG, 20 mM) (n = 5). *** $p < 0.001$, Student's t test.

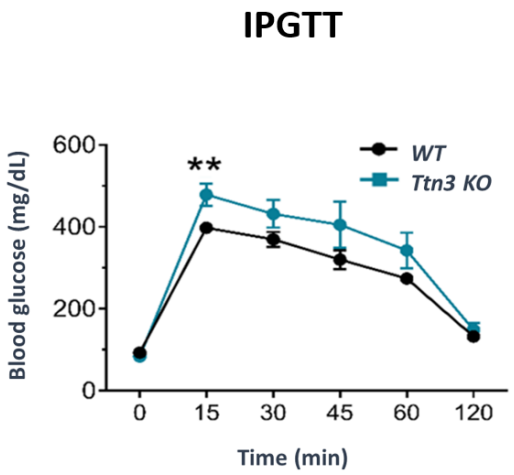

Figure 28. *Ttn3* KO mice show higher blood glucose level

Intraperitoneal glucose tolerance (IPGTT). The level of glucose in serum were measured in 16hr fasting WT and *Ttn3* KO mice before and after glucose injection (2 g/kg body weight) (*n* = 7-9). ** $p < 0.01$, Student's *t* test.

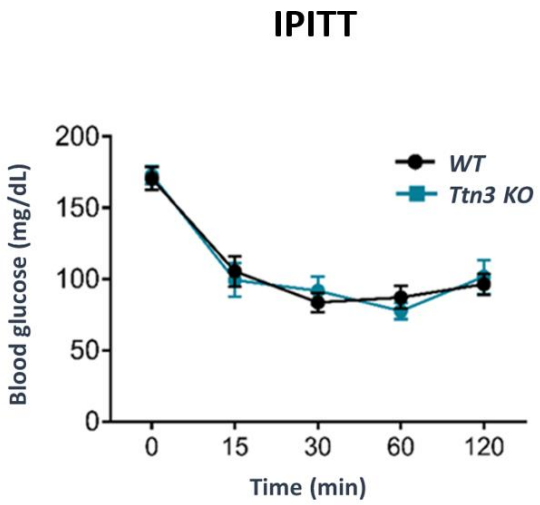

Figure 29. Sensitivity to Insulin is preserved in *Ttn3* KO mice

Intraperitoneal insulin tolerance (IPITT). The level of glucose in serum were measured in 6hr fasting WT and *Ttn3* KO mice before and after insulin injection (0.5U / body weight) (*n* = 8 / genotype). ** $p < 0.01$, Student's *t* test.

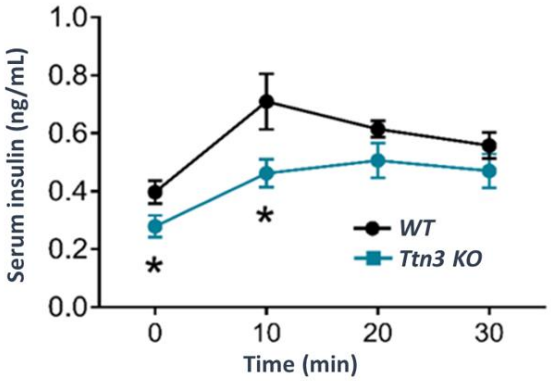

Figure 30. Decreased insulin secretion in *Ttn3* KO mice

Glucose-stimulated insulin secretion. The levels of insulin in serum were measured in WT and *Ttn3* KO mice at every 10 min after the administration of glucose (2 g/kg body weight) (n = 14 / genotype). * $p < 0.05$, Student's t test

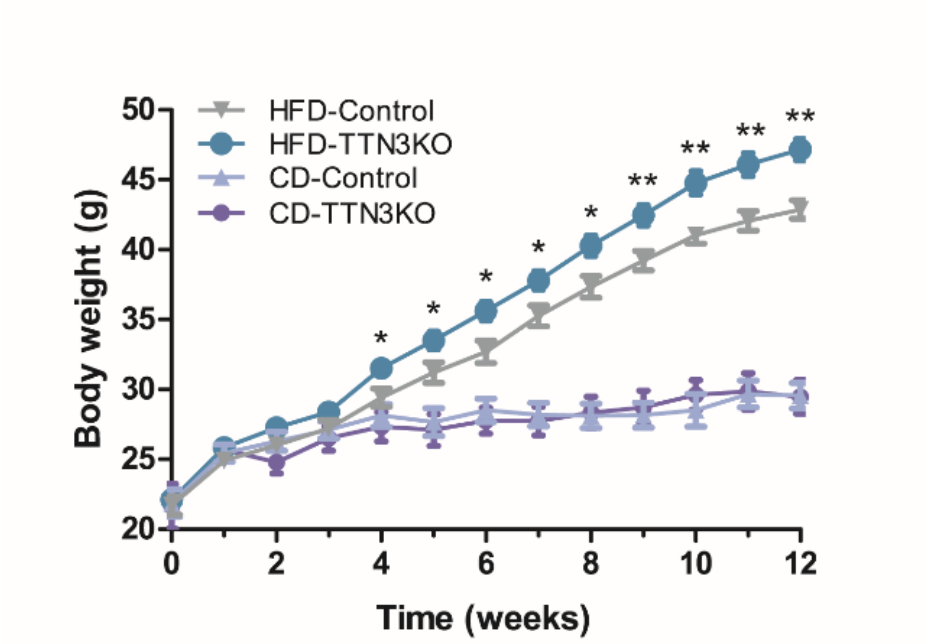

Figure 31. Effects of HFD on body weight in *Ttn3* KO mice

WT and *Ttn3* KO mice were placed on high fat diet (HFD), or the nutritionally matched low fat control diet (CD) for 12 weeks. Mice were weighted once a week. (*n* = 5-6 / CD, *n* = 8-11 / HFD). * $p < 0.05$, ** $p < 0.05$, Student's *t* test

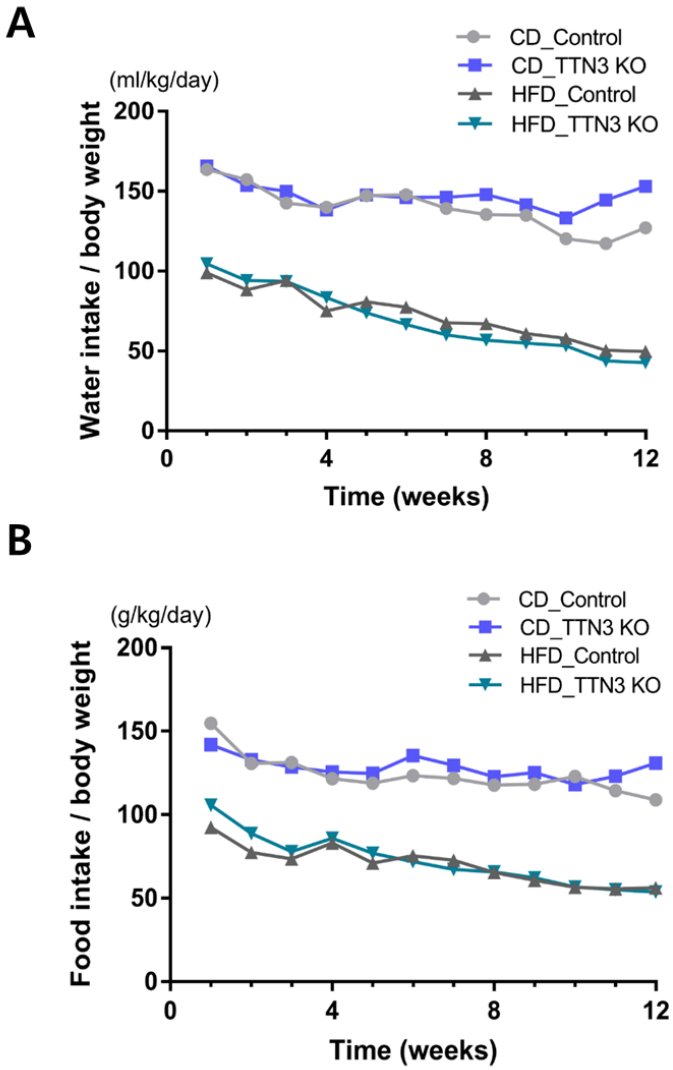

Figure 32. Time course of food intake and water intake during HFD

Discussion

Glucose homeostasis is tightly regulated by pancreatic endocrine hormones, insulin and glucagon, which lowers and raises blood glucose, respectively. Not like other parts of the body, the brain cannot store glucose and mostly depends on the glucose in the bloodstream (12). Therefore, it is important to maintain a constant level of blood glucose, which process is known as glucose homeostasis. Diabetes mellitus is a metabolic disease that the blood glucose level is not maintained within a controlled range due to impaired insulin sensitivity or insufficient insulin secretion from pancreatic β-cells (30, 31). Moreover it is followed by severe complications such as retinopathy, neuropathy, nephropathy and atherosclerosis (35). Molecular mechanisms underlying the glucose-stimulated insulin secretion in pancreatic β-cells have been studied intensely. The involvement of K_{ATP} channel in the insulin secretion becomes the leading pathway for the glucose-stimulated insulin secretion. However, an alternative pathway for the glucose-stimulated insulin secretion are also suggested (62-65). SAC channel activity is suggested for one of the alternative mechanisms for the glucose-stimulated insulin secretion (65, 69). The molecular identity of SAC channel, however, remained unknown. In the present study, we suggest that TTN3 is an additional regulator for glucose-stimulated insulin secretion in pancreatic β-cells (Figure 33): (1) its

selective expression in β-cells, (2) TTN3-like mechanosensitive currents in pancreatic β-cells, (3) genetic ablation of *Ttn3* in pancreatic β-cells leads to decreased Ca^{2+} influx and electrical activity in response to glucose stimulation, and (4) *Ttn3* gene deletion leads to impaired glucose tolerance with decreased insulin secretion *in vivo*.

Glucose-stimulated insulin secretion is regulated by cytoplasmic concentration of Ca^{2+}, which mediates membrane docking, tethering and exocytosis of insulin granules (111). A number of studies unveiled the mechanism of Ca^{2+} signaling in pancreatic β-cells upon glucose stimulation (56, 112). The source of intracellular Ca^{2+} increase is the extracellular Ca^{2+} through voltage-gated Ca^{2+} channel, which is activated by β-cell depolarization (113, 114). The major component responsible for the β-cell depolarization is thought to be the closure of K_{ATP} channels (115). However, several studies suggest that the K_{ATP} channel is not the sole ionic mechanism underlying the depolarization and predict the presence of additional contributors for the depolarization of β-cells(58, 62, 116). In line with this notion, swelling of the β-cells induced by glucose is also considered as a significant factor stimulating insulin secretion (65, 71). Exposed to high concentration of glucose, glycolysis in the β-cells is accelerated and leads to an intracellular lactate accumulation (71, 73, 117). The accumulation of lactate results in intracellular hyper-osmolality that draws water via aquaporin 7 into the cell (79, 118, 119). Even in the absence of glucose, osmotic swelling of β-cells induced insulin secretion (62, 64, 72). Thus, swelling itself is one

of the triggering pathways to insulin secretion.

The role of volume-regulated anion channel (VRAC) in β-cells has been studied (69-71). VRAC can depolarize β-cells because they mediate the efflux of anion, Cl^-. In fact, the equilibrium potential of Cl^- is relatively high (-30 mV) in β-cells, which leads to the depolarization of the cell(64, 120). The molecular identity of the VRAC was identified to be SWELL1/LRRC8a (121). Recently, it has been shown that SWELL1 has an important role in glucose sensing and therefore enhancing insulin secretion as SWELL1 deficient mice showed impaired glucose tolerance and insulin secretion (83, 84).

The presence of SAC channels along with the VRAC in pancreatic β-cells has been also suggested as their blockers such as gadolinium, amiloride, 2-APB, and ruthenium red inhibit the swelling-stimulated insulin secretion in β-cells (65, 69). In addition, the treatment of anion channel blockers to β-cells partially blocked the swelling-induced Ca^{2+} influx or insulin secretion (85, 86). The present study showed that mechanical step stimuli evoked currents with slow inactivation kinetics that are absent in β-cells of *Ttn3* KO mice. *Ttn3* overexpressing cells responded to hypotonic solution. Cationic currents and intracellular Ca^{2+} increase evoked by hypotonic solution were markedly reduced in *Ttn3* deficient β-cells. Thus, these data suggest that TTN3 may be a key component of SAC channels in β-cells, which sense mechanical tension of the plasma membrane and transduce it to electrical activity β-cells.

TTN3 has been recently determined as a mechanosensitive non-selective cation channel (78). In addition, independency of TTN3's function as a mechanosensor was questioned (122, 123). Here, the dependency of TTN3 on Piezo1 may also be questioned, but recent study determined that Piezo1 is expressed in acinar cells and is involved in pancreatitis (124). In addition, immunohistochemistry staining for Piezo1 in mouse pancreatic tissue revealed that Piezo 1 is not expressed in insulin-secreting β-cells (Figure 34). Therefore, the role of TTN3 in pancreatic β-cells as a mechanosensor and a mediator of Ca^{2+} influx supports the independency of TTN3 in mechanotransduction.

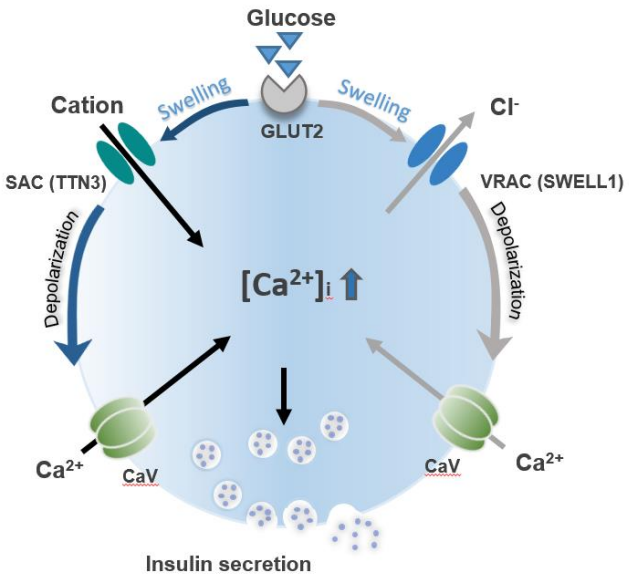

Figure 33. Mechanism of swelling-stimulated insulin secretion in β-cells through TTN3

Schematic illustration shows high concentration of glucose initially evokes β-cell inflation, which then activates VRCC (cyan, e.g. TTN3) and VRAC (blue, e.g. SWELL1), respectively. TTN3 alone mediates cationic influx into the cell. Also, influx of cations (black arrow) and efflux of chloride ions (grey arrow) depolarize the cell membrane leading to VGCC activation. These cellular events increase cytosolic Ca^{2+} concentration promoting insulin vesicle fusion and insulin release in pancreatic β-cells (Bold blue arrows) depict a novel mechanism of TTN3 in glucose-induced swelling-stimulated insulin secretion.

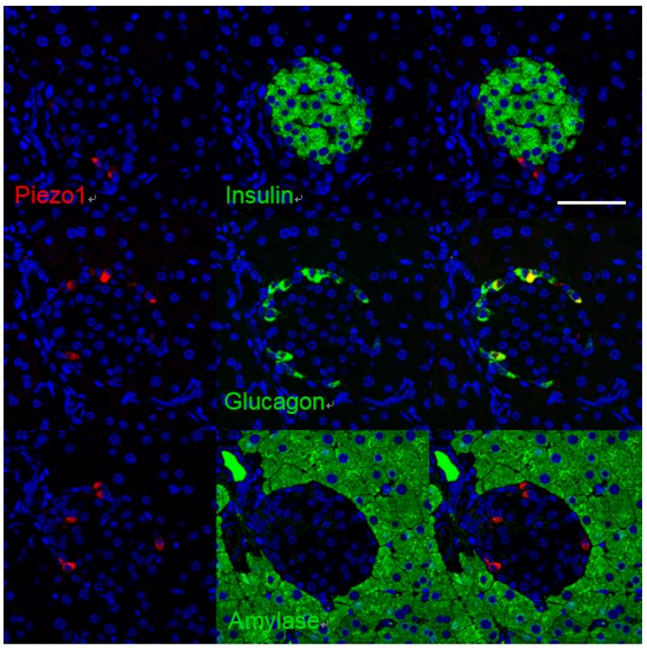

Figure 34. Immunofluorescence analysis of Piezo1 in mouse pancreas

Immunofluorescence staining of mPiezo1 (red) and insulin (green, upper panels), glucagon (green, middle panels), or amylase (green, lower panels) in mouse pancreas sections. Scale bar represents 50 µm.

Conclusion

We questioned whether TTN3 contributes to the depolarization evoked by glucose-induced swelling in pancreatic β-cells. Using immunohistochemistry, we observed its expression in mouse pancreatic β-cells. Electrophysiological studies revealed that TTN3 mediates cationic currents in response to the hypotonicity-induced and high glucose-induced swelling in pancreatic β-cells. TTN3 activation by swelling and high glucose evoked depolarization along with the electrical activities in β-cells. Independent of K_{ATP}-channel and VRAC channel mediated pathway, increase in Ca^{2+} influx was also observed upon hypotonic and glucose stimulations. In addition, ablation of *Ttn3* resulted in impaired glucose tolerance with decreased insulin secretion. Consequently, in this study we suggest that TTN3 mediates swelling-stimulated cationic currents in pancreatic β-cells and regulates glucose-stimulated insulin secretion.

References

1. Holt RI, Cockram C, Flyvbjerg A, and Goldstein BJ. *Textbook of diabetes.* John Wiley & Sons; 2017.

2. Glucose | Origin and meaning of glucose by Online Etymology Dictionary. 2018.

3. What is Blood Sugar? 2009.

4. Poretsky L. *Principles of diabetes mellitus.* New York: Springer; 2010.

5. Calle-Pascual AL, Marenco G, Asis MJ, Bordiu E, Romeo S, Romero C, et al. Effects of different proportions of carbohydrates, polysaccharides/monosaccharides, and different fibers on the metabolic control in diabetic rats. *Metabolism.* 1986;35(10):919-23.

6. The Endocrine Pancreas Anatomy and Physiology. https://opentextbc.ca/anatomyandphysiology/chapter/17-9-the-endocrine-pancreas.

7. Feher J. In: Feher J ed. *Quantitative Human Physiology*. Boston: Academic Press; 2012:171-9.

8. Meinke MH, and Edstrom RD. Muscle glycogenolysis. Regulation of the cyclic interconversion of phosphorylase a and phosphorylase b. *J Biol Chem.* 1991;266(4):2259-66.

9. Bhagavan NV, and Ha C-E. In: Bhagavan NV, and Ha C-E eds. *Essentials of Medical Biochemistry*. San Diego: Academic Press; 2011:151-68.

10. Brown GC. Control of respiration and ATP synthesis in mammalian mitochondria and cells. *Biochem J.* 1992;284 (Pt 1):1-13.

11. Gerich JE. Control of glycaemia. *Baillieres Clin Endocrinol Metab.* 1993;7(3):551-86.

12. Mergenthaler P, Lindauer U, Dienel GA, and Meisel A. Sugar for the brain: the role of glucose in physiological and pathological brain function. *Trends Neurosci.* 2013;36(10):587-97.

13. Henderson ST. Ketone bodies as a therapeutic for Alzheimer's disease. *Neurotherapeutics : the journal of the American Society for Experimental NeuroTherapeutics.* 2008;5(3):470-80.

14. Feeding the Diabetic Brain | Penn State University. 2018.

15. Trucco M. Regeneration of the pancreatic beta cell. *J Clin Invest.*

2005;115(1):5-12.

16. Roder PV, Wu B, Liu Y, and Han W. Pancreatic regulation of glucose homeostasis. *Exp Mol Med.* 2016;48:e219.

17. Aronoff SL, Berkowitz K, Shreiner B, and Want L. Glucose Metabolism and Regulation: Beyond Insulin and Glucagon. *Diabetes Spectrum.* 2004;17(3):183-90.

18. *Joslin's Diabetes Mellitus.* Lippincott WIlliams & Wilkins; 2005.

19. L. Aronoff S, Berkowitz KB, Barb Shreiner B, and Want L. *Glucose Metabolism and Regulation: Beyond Insulin and Glucagon.* 2004.

20. Adeva-Andany MM, Gonzalez-Lucan M, Donapetry-Garcia C, Fernandez-Fernandez C, and Ameneiros-Rodriguez E. Glycogen metabolism in humans. *BBA Clin.* 2016;5:85-100.

21. American Diabetes A. Diagnosis and classification of diabetes mellitus. *Diabetes Care.* 2009;32 Suppl 1:S62-7.

22. Liamis G, Liberopoulos E, Barkas F, and Elisaf M. Diabetes mellitus and electrolyte disorders. *World J Clin Cases.* 2014;2(10):488-96.

23. Sircar M, Bhatia A, and Munshi M. Review of Hypoglycemia in the Older Adult: Clinical Implications and Management. *Can J Diabetes.* 2016;40(1):66-72.

24. Samuel VT, and Shulman GI. The pathogenesis of insulin resistance: integrating signaling pathways and substrate flux. *J Clin Invest.* 2016;126(1):12-22.

25. Kasuga M. Insulin resistance and pancreatic beta cell failure. *J Clin Invest.* 2006;116(7):1756-60.

26. Alsahli M, Z. Shrayyef M, and E. Gerich J. 2017:1-20.

27. Strowski MZ, Parmar RM, Blake AD, and Schaeffer JM. Somatostatin inhibits insulin and glucagon secretion via two receptors subtypes: an in vitro study of pancreatic islets from somatostatin receptor 2 knockout mice. *Endocrinology.* 2000;141(1):111-7.

28. Weir GC, Samols E, Loo S, Patel YC, and Gabbay KH. Somatostatin and pancreatic polypeptide secretion: effects of glucagon, insulin, and arginine. *Diabetes.* 1979;28(1):35-40.

29. LeRoith D. Beta-cell dysfunction and insulin resistance in type 2 diabetes: role of metabolic and genetic abnormalities. *Am J Med.* 2002;113 Suppl 6A:3S-11S.

30. Ashcroft FM, and Rorsman P. Diabetes Mellitus and the beta Cell: The Last Ten Years. *Cell.* 2012;148(6):1160-71.

31. Porte D, Jr., and Kahn SE. beta-cell dysfunction and failure in type 2 diabetes: potential mechanisms. *Diabetes.* 2001;50 Suppl 1:S160-3.

32. Kharroubi AT, and Darwish HM. Diabetes mellitus: The epidemic of the century. *World J Diabetes.* 2015;6(6):850-67.

33. Kahn SE. The importance of the beta-cell in the pathogenesis of type 2 diabetes mellitus. *Am J Med.* 2000;108 Suppl 6a:2S-8S.

34. Mathers CD, and Loncar D. Projections of global mortality and burden of disease from 2002 to 2030. *PLoS Med.* 2006;3(11):e442.

35. Zheng Y, Ley SH, and Hu FB. Global aetiology and epidemiology of type 2 diabetes mellitus and its complications. *Nat Rev Endocrinol.* 2018;14(2):88-98.

36. Zhuo X, Zhang P, and Hoerger TJ. Lifetime direct medical costs of treating type 2 diabetes and diabetic complications. *Am J Prev Med.* 2013;45(3):253-61.

37. Galtier F. Definition, epidemiology, risk factors. *Diabetes Metab.* 2010;36(6 Pt 2):628-51.

38. 2. Classification and Diagnosis of Diabetes: Standards of Medical Care in Diabetes-2018. *Diabetes Care.* 2018;41(Suppl 1):S13-s27.

39. Maahs DM, West NA, Lawrence JM, and Mayer-Davis EJ. Epidemiology of type 1 diabetes. *Endocrinol Metab Clin North Am.* 2010;39(3):481-97.

40. Dabelea D, Mayer-Davis EJ, Saydah S, Imperatore G, Linder B, Divers J, et al. Prevalence of type 1 and type 2 diabetes among children and adolescents from 2001 to 2009. *Jama.* 2014;311(17):1778-86.

41. American Diabetes A. 2. Classification and Diagnosis of Diabetes: Standards of Medical Care in Diabetes-2018. *Diabetes Care.* 2018;41(Suppl 1):S13-S27.

42. Komatsu M, Takei M, Ishii H, and Sato Y. Glucose-stimulated insulin secretion: A newer perspective. *J Diabetes Investig.* 2013;4(6):511-6.

43. Ammala C, Larsson O, Berggren PO, Bokvist K, Juntti-Berggren L, Kindmark H, et al. Inositol trisphosphate-dependent periodic activation of a Ca(2+)-activated K+ conductance in glucose-stimulated pancreatic beta-cells. *Nature.* 1991;353(6347):849-52.

44. Atouf F, Czernichow P, and Scharfmann R. Expression of neuronal traits in pancreatic beta cells. Implication of neuron-restrictive silencing factor/repressor element silencing transcription factor, a neuron-restrictive silencer. *J Biol Chem.* 1997;272(3):1929-34.

45. Baekkeskov S, Aanstoot H-J, Christgai S, Reetz A, Solimena M,

Cascalho M, et al. Identification of the 64K autoantigen in insulin-dependent diabetes as the GABA-synthesizing enzyme glutamic acid decarboxylase. *Nature.* 1990;347(6289):151.

46. Teitelman G, and Lee J. Cell lineage analysis of pancreatic islet cell development: glucagon and insulin cells arise from catecholaminergic precursors present in the pancreatic duct. *Developmental biology.* 1987;121(2):454-66.

47. Watanabe T, and Nagatsu I. Immunohistochemical colocalization of insulin, aromatic L-amino acid decarboxylase and dopamine beta-hydroxylase in islet B cells of chicken pancreas. *Cell and tissue research.* 1991;263(1):131-6.

48. Philipson LH, Kusnetsov A, Larson T, Zeng Y, and Westermark G. Human, Rodent, and Canine Pancreatic β-cells Express a Sodium Channel α₁-Subunit Related to a Fetal Brain Isoform. *Diabetes.* 1993;42(9):1372-7.

49. Gonoi T, Mizuno N, Inagaki N, Kuromi H, Seino Y, Miyazaki J, et al. Functional neuronal ionotropic glutamate receptors are expressed in the non-neuronal cell line MIN6. *J Biol Chem.* 1994;269(25):16989-92.

50. Teitelman G. Insulin cells of pancreas extend neurites but do not arise from the neuroectoderm. *Developmental biology.* 1990;142(2):368-79.

51. Atouf F, Tazi A, Polak M, Czemichow P, and Scharfmann R. Dexamethasone regulates the expression of neuronal properties of a rat insulinoma cell line. *Journal of neuroendocrinology.* 1995;7(12):957-64.

52. Scharfmann R, Tazi A, Polak M, Kanaka C, and Czernichow P. Expression of Functional Nerve Growth Factor Receptors in Pancreatic β-cell Lines and Fetal Rat Islets in Primary Culture. *Diabetes.* 1993;42(12):1829-36.

53. Polak M, Scharfmann R, Seilheimer B, Eisenbarth G, Dressler D, Verma IM, et al. Nerve growth factor induces neuron-like differentiation of an insulin-secreting pancreatic beta cell line. *Proceedings of the National Academy of Sciences.* 1993;90(12):5781-5.

54. Scharfmann R, ARATAN-SPIRE S, DUBOIS P, BASMACIOGULLARI A, and Czernichow P. Persistence of peptidylglycine α-amidating monooxygenase activity and elevated thyrotropin-releasing hormone concentrations in fetal rat islets in culture. *Endocrinology.* 1988;123(3):1329-34.

55. Martino E, Seo H, Lernmark A, and Refetoff S. Ontogenetic patterns of thyrotropin-releasing hormone-like material in rat hypothalamus, pancreas, and retina: selective effect of light deprivation. *Proceedings*

of the National Academy of Sciences. 1980;77(7):4345-8.

56. Rorsman P, and Ashcroft FM. Pancreatic beta-Cell Electrical Activity and Insulin Secretion: Of Mice and Men. *Physiol Rev.* 2018;98(1):117-214.

57. Dean PM, and Matthews EK. Electrical activity in pancreatic islet cells. *Nature.* 1968;219(5152):389-90.

58. Ashcroft FM, Harrison DE, and Ashcroft SJ. Glucose induces closure of single potassium channels in isolated rat pancreatic beta-cells. *Nature.* 1984;312(5993):446-8.

59. Cook DL, and Hales CN. Intracellular ATP directly blocks K+ channels in pancreatic B-cells. *Nature.* 1984;311(5983):271-3.

60. Colsoul B, Schraenen A, Lemaire K, Quintens R, Van Lommel L, Segal A, et al. Loss of high-frequency glucose-induced Ca2+ oscillations in pancreatic islets correlates with impaired glucose tolerance in Trpm5-/- mice. *Proc Natl Acad Sci U S A.* 2010;107(11):5208-13.

61. MacDonald PE, Joseph JW, and Rorsman P. Glucose-sensing mechanisms in pancreatic beta-cells. *Philos Trans R Soc Lond B Biol Sci.* 2005;360(1464):2211-25.

62. Blackard WG, Kikuchi M, Rabinovitch A, and Renold AE. An effect of hyposmolarity on insulin release in vitro. *Am J Physiol.* 1975;228(3):706-13.

63. Gembal M, Gilon P, and Henquin JC. Evidence that glucose can control insulin release independently from its action on ATP-sensitive K+ channels in mouse B cells. *J Clin Invest.* 1992;89(4):1288-95.

64. Drews G, Zempel G, Krippeit-Drews P, Britsch S, Busch GL, Kaba NK, et al. Ion channels involved in insulin release are activated by osmotic swelling of pancreatic B-cells. *Biochim Biophys Acta.* 1998;1370(1):8-16.

65. Takii M, Ishikawa T, Tsuda H, Kanatani K, Sunouchi T, Kaneko Y, et al. Involvement of stretch-activated cation channels in hypotonically induced insulin secretion in rat pancreatic beta-cells. *Am J Physiol Cell Physiol.* 2006;291(6):C1405-11.

66. Ravier MA, Nenquin M, Miki T, Seino S, and Henquin JC. Glucose controls cytosolic Ca2+ and insulin secretion in mouse islets lacking adenosine triphosphate-sensitive K+ channels owing to a knockout of the pore-forming subunit Kir6.2. *Endocrinology.* 2009;150(1):33-45.

67. Eliasson L, Ma X, Renstrom E, Barg S, Berggren PO, Galvanovskis J, et al. SUR1 regulates PKA-independent cAMP-induced granule priming in mouse pancreatic B-cells. *J Gen Physiol.* 2003;121(3):181-

97.

68. Haspel D, Krippeit-Drews P, Aguilar-Bryan L, Bryan J, Drews G, and Dufer M. Crosstalk between membrane potential and cytosolic Ca2+ concentration in beta cells from Sur1-/- mice. *Diabetologia.* 2005;48(5):913-21.

69. Nakayama K, Tanabe Y, Obara K, and Ishikawa T. In: Kamkin A, and Lozinsky I eds. *Mechanically Gated Channels and their Regulation*. Dordrecht: Springer Netherlands; 2012:379-404.

70. Semino MC, Gagliardino AM, Bianchi C, Rebolledo OR, and Gagliardino JJ. Early changes in the rat pancreatic B cell size induced by glucose. *Acta Anat (Basel).* 1990;138(4):293-6.

71. Miley HE, Sheader EA, Brown PD, and Best L. Glucose-induced swelling in rat pancreatic beta-cells. *J Physiol.* 1997;504 (Pt 1):191-8.

72. Best L, Miley HE, and Yates AP. Activation of an anion conductance and beta-cell depolarization during hypotonically induced insulin release. *Exp Physiol.* 1996;81(6):927-33.

73. Davies SL, Brown PD, and Best L. Glucose-induced swelling in rat pancreatic alpha-cells. *Mol Cell Endocrinol.* 2007;264(1-2):61-7.

74. Jaalouk DE, and Lammerding J. Mechanotransduction gone awry. *Nat Rev Mol Cell Biol.* 2009;10(1):63-73.

75. French AS. Mechanotransduction. *Annu Rev Physiol.* 1992;54:135-52.

76. Martinac B, and Poole K. Mechanically activated ion channels. *Int J Biochem Cell Biol.* 2018;97:104-7.

77. Geffeney Shana L, and Goodman Miriam B. How We Feel: Ion Channel Partnerships that Detect Mechanical Inputs and Give Rise to Touch and Pain Perception. *Neuron.* 2012;74(4):609-19.

78. Hong GS, Lee B, Wee J, Chun H, Kim H, Jung J, et al. Tentonin 3/TMEM150c Confers Distinct Mechanosensitive Currents in Dorsal-Root Ganglion Neurons with Proprioceptive Function. *Neuron.* 2016;91(3):708-10.

79. Sekine N, Cirulli V, Regazzi R, Brown LJ, Gine E, Tamarit-Rodriguez J, et al. Low lactate dehydrogenase and high mitochondrial glycerol phosphate dehydrogenase in pancreatic beta-cells. Potential role in nutrient sensing. *J Biol Chem.* 1994;269(7):4895-902.

80. Best L, Miley HE, Brown PD, and Cook LJ. Methylglyoxal causes swelling and activation of a volume-sensitive anion conductance in rat pancreatic beta-cells. *J Membr Biol.* 1999;167(1):65-71.

81. Best L. Study of a glucose-activated anion-selective channel in rat

pancreatic beta-cells. *Pflugers Arch.* 2002;445(1):97-104.

82. Best L, Yates AP, Decher N, Steinmeyer K, and Nilius B. Inhibition of glucose-induced electrical activity in rat pancreatic beta-cells by DCPIB, a selective inhibitor of volume-sensitive anion currents. *Eur J Pharmacol.* 2004;489(1-2):13-9.

83. Kang C, Xie L, Gunasekar SK, Mishra A, Zhang Y, Pai S, et al. SWELL1 is a glucose sensor regulating beta-cell excitability and systemic glycaemia. *Nat Commun.* 2018;9(1):367.

84. Stuhlmann T, Planells-Cases R, and Jentsch TJ. LRRC8/VRAC anion channels enhance beta-cell glucose sensing and insulin secretion. *Nat Commun.* 2018;9(1):1974.

85. Kinard TA, Goforth PB, Tao Q, Abood ME, Teague J, and Satin LS. Chloride channels regulate HIT cell volume but cannot fully account for swelling-induced insulin secretion. *Diabetes.* 2001;50(5):992-1003.

86. Straub SG, and Sharp GW. Glucose-stimulated signaling pathways in biphasic insulin secretion. *Diabetes Metab Res Rev.* 2002;18(6):451-63.

87. Casas S, Novials A, Reimann F, Gomis R, and Gribble FM. Calcium elevation in mouse pancreatic beta cells evoked by extracellular human islet amyloid polypeptide involves activation of the mechanosensitive ion channel TRPV4. *Diabetologia.* 2008;51(12):2252-62.

88. Hisanaga E, Nagasawa M, Ueki K, Kulkarni RN, Mori M, and Kojima I. Regulation of calcium-permeable TRPV2 channel by insulin in pancreatic beta-cells. *Diabetes.* 2009;58(1):174-84.

89. Pruszynski JA, Kurtzer I, Nashed JY, Omrani M, Brouwer B, and Scott SH. Primary motor cortex underlies multi-joint integration for fast feedback control. *Nature.* 2011;478(7369):387-90.

90. Kim S, Yun HM, Baik JH, Chung KC, Nah SY, and Rhim H. Functional interaction of neuronal Cav1.3 L-type calcium channel with ryanodine receptor type 2 in the rat hippocampus. *J Biol Chem.* 2007;282(45):32877-89.

91. Best L, and Brown PD. Studies of the mechanism of activation of the volume-regulated anion channel in rat pancreatic beta-cells. *J Membr Biol.* 2009;230(2):83-91.

92. Majid A, Speake T, Best L, and Brown PD. Expression of the Na+K+-2Cl- cotransporter in alpha and beta cells isolated from the rat pancreas. *Pflugers Arch.* 2001;442(4):570-6.

93. Gopel SO, Kanno T, Barg S, and Rorsman P. Patch-clamp characterisation of somatostatin-secreting -cells in intact mouse

pancreatic islets. *J Physiol.* 2000;528(Pt 3):497-507.

94. Gopel SO, Kanno T, Barg S, Weng XG, Gromada J, and Rorsman P. Regulation of glucagon release in mouse -cells by KATP channels and inactivation of TTX-sensitive Na+ channels. *J Physiol.* 2000;528(Pt 3):509-20.

95. Cacace VI, Finkelsteyn AG, Tasso LM, Kusnier CF, Gomez KA, and Fischbarg J. Regulatory volume increase and regulatory volume decrease responses in HL-1 atrial myocytes. *Cell Physiol Biochem.* 2014;33(6):1745-57.

96. Sardini A, Amey JS, Weylandt KH, Nobles M, Valverde MA, and Higgins CF. Cell volume regulation and swelling-activated chloride channels. *Biochim Biophys Acta.* 2003;1618(2):153-62.

97. Eggermont J, Trouet D, Carton I, and Nilius B. Cellular function and control of volume-regulated anion channels. *Cell Biochem Biophys.* 2001;35(3):263-74.

98. Maertens C, Wei L, Voets T, Droogmans G, and Nilius B. Block by fluoxetine of volume-regulated anion channels. *Br J Pharmacol.* 1999;126(2):508-14.

99. McLarnon JG, Helm J, Goghari V, Franciosi S, Choi HB, Nagai A, et al. Anion channels modulate store-operated calcium influx in human microglia. *Cell Calcium.* 2000;28(4):261-8.

100. Ashcroft FM, and Rorsman P. Electrophysiology of the pancreatic beta-cell. *Prog Biophys Mol Biol.* 1989;54(2):87-143.

101. Nichols CG. KATP channels as molecular sensors of cellular metabolism. *Nature.* 2006;440(7083):470-6.

102. Drews G, Krippeit-Drews P, and Dufer M. Electrophysiology of islet cells. *Adv Exp Med Biol.* 2010;654:115-63.

103. Best L. Glucose-induced electrical activity in rat pancreatic beta-cells: dependence on intracellular chloride concentration. *J Physiol.* 2005;568(Pt 1):137-44.

104. Daniel S, Noda M, Straub SG, and Sharp GW. Identification of the docked granule pool responsible for the first phase of glucose-stimulated insulin secretion. *Diabetes.* 1999;48(9):1686-90.

105. Gaisano HY. Here come the newcomer granules, better late than never. *Trends Endocrinol Metab.* 2014;25(8):381-8.

106. Hou JC, Min L, and Pessin JE. Insulin granule biogenesis, trafficking and exocytosis. *Vitam Horm.* 2009;80:473-506.

107. Tang J, Maximov A, Shin OH, Dai H, Rizo J, and Sudhof TC. A

complexin/synaptotagmin 1 switch controls fast synaptic vesicle exocytosis. *Cell.* 2006;126(6):1175-87.

108. Ashcroft FM, and Rorsman P. ATP-sensitive K+ channels: a link between B-cell metabolism and insulin secretion. *Biochem Soc Trans.* 1990;18(1):109-11.

109. Guldstrand M, Grill V, Bjorklund A, Lins PE, and Adamson U. Improved beta cell function after short-term treatment with diazoxide in obese subjects with type 2 diabetes. *Diabetes Metab.* 2002;28(6 Pt 1):448-56.

110. Obrosova IG, Ilnytska O, Lyzogubov VV, Pavlov IA, Mashtalir N, Nadler JL, et al. High-fat diet induced neuropathy of pre-diabetes and obesity: effects of "healthy" diet and aldose reductase inhibition. *Diabetes.* 2007;56(10):2598-608.

111. Kohnert KD, Hahn HJ, Gylfe E, Borg H, and Hellman B. Calcium and pancreatic beta-cell function. 6. Glucose and intracellular 45Ca distribution. *Mol Cell Endocrinol.* 1979;16(3):205-20.

112. Wollheim CB, and Sharp GW. Regulation of insulin release by calcium. *Physiol Rev.* 1981;61(4):914-73.

113. Worley JF, 3rd, McIntyre MS, Spencer B, Mertz RJ, Roe MW, and Dukes ID. Endoplasmic reticulum calcium store regulates membrane potential in mouse islet beta-cells. *J Biol Chem.* 1994;269(20):14359-62.

114. Yang SN, and Berggren PO. CaV2.3 channel and PKClambda: new players in insulin secretion. *J Clin Invest.* 2005;115(1):16-20.

115. Seghers V, Nakazaki M, DeMayo F, Aguilar-Bryan L, and Bryan J. Sur1 knockout mice. A model for K(ATP) channel-independent regulation of insulin secretion. *J Biol Chem.* 2000;275(13):9270-7.

116. Best L. Evidence that glucose-induced electrical activity in rat pancreatic beta-cells does not require KATP channel inhibition. *J Membr Biol.* 2002;185(3):193-200.

117. Best L, Trebilcock R, and Tomlinson S. Lactate transport in insulin-secreting beta-cells: contrast between rat islets and HIT-T15 insulinoma cells. *Mol Cell Endocrinol.* 1992;86(1-2):49-56.

118. Best L, Yates AP, and Tomlinson S. Stimulation of insulin secretion by glucose in the absence of diminished potassium (86Rb+) permeability. *Biochem Pharmacol.* 1992;43(11):2483-5.

119. Louchami K, Best L, Brown P, Virreira M, Hupkens E, Perret J, et al. A new role for aquaporin 7 in insulin secretion. *Cell Physiol Biochem.* 2012;29(1-2):65-74.

120. Kinard TA, and Satin LS. An ATP-sensitive Cl- channel current that is activated by cell swelling, cAMP, and glyburide in insulin-secreting cells. *Diabetes.* 1995;44(12):1461-6.

121. Qiu Z, Dubin AE, Mathur J, Tu B, Reddy K, Miraglia LJ, et al. SWELL1, a plasma membrane protein, is an essential component of volume-regulated anion channel. *Cell.* 2014;157(2):447-58.

122. Dubin AE, Murthy S, Lewis AH, Brosse L, Cahalan SM, Grandl J, et al. Endogenous Piezo1 Can Confound Mechanically Activated Channel Identification and Characterization. *Neuron.* 2017;94(2):266-70.e3.

123. Hong GS, Lee B, and Oh U. Evidence for Mechanosensitive Channel Activity of Tentonin 3/TMEM150C. *Neuron.* 2017;94(2):271-3 e2.

124. Romac JM, Shahid RA, Swain SM, Vigna SR, and Liddle RA. Piezo1 is a mechanically activated ion channel and mediates pressure induced pancreatitis. *Nat Commun.* 2018;9(1):1715.

국 문 초 록

포도당은 인체의 에너지원으로 중요한 물질이다. 세포는 해당과정(glycolysis)과 미토콘드리아 내 유기호흡을 통해 포도당을 인체의 에너지 형태인 ATP (아데노신 삼인산)로 합성한다. 과다하게 섭취된 포도당은 호르몬 인슐린에 의해 글리코겐이라는 형태로 간에 저장되어 혈당이 떨어지는 경우, 호르몬 글루코겐에 의해 다시 포도당으로 전환 되어 혈액을 통하여 다른 세포들에게 전달된다. 하지만 뇌와 같은 장기는 혈액 내 포도당에만 의존하여 에너지를 공급 받기에 혈액 내 일정한 포도당 농도를 유지하는 것이 뇌의 기능을 위해 중요하다.

당항상성은 주로 췌장에서 분비 되는 호르몬에 의해 조절된다. 혈당의 높낮이는 췌장 내 랑게르한스섬에 의해 감지 되어 호르몬들이 분비되는데, 저혈당의 경우 글루카곤이, 고혈당의 경우 인슐린이 분비된다. 췌장 베타세포에서 인슐린 분비 기전으로는 ATP-sensitive potassium (K_{ATP}) 채널에 의존하는 기전이 가장 잘 알려져 있다. 혈액 내 포도당은 췌장 베타세포의 운반체인 GLUT2 (Glucose transporter)를 통해 세포 내로 유입되어 대사과정에 의해 ATP가 생성되는데, ATP의 증가는 K_{ATP} 채널의 통로를 닫는다. 칼륨(K)이 세포 내에 축적 되면 세포막의 탈분극이 일어나고, 이는 전압의존성 칼슘채널을 열어 세포내 칼슘 농도를 증가시킨다.

칼슘은 인슐린과 세포막의 융합을 유도하여 세포외배출을 일으킨다. 하지만 이와 더불어 K_{ATP} 채널에 의존하지 않는 또 다른 인슐린 분비 기전이 존재한다는 것이 알려져 있다. 고농도의 포도당이 대사전달에서 생성되는 젖산에 의해 삼투압에 따른 세포 팽창을 일으키고, 세포막의 수축에 따라 부피 감지 음이온채널 및 기계적 자극 감지 양이온채널들을 활성화 시킬 것이라고 알려져 있지만 이들의 분자적 정보는 잘 알려져 있지 않다.

최근 우리 실험실에서는 오감각의 하나인 촉각, 즉 기계적인 자극에 의해 조절되는 양이온 전류가 TMEM150C/Tentonin 3(TTN3) 채널에 의해 조절된다는 것을 밝혔다. 선행연구에서 TTN3 단백질이 췌장에서 높은 발현을 보이는 것을 확인하였다. 기계적 자극을 감지하는 채널인 TTN3가 췌장 내에서 어떠한 영향을 미치는지 알아보고자 본 연구를 시작하게 되었다. 결과로, TTN3가 췌장 내 인슐린을 분비하는 베타세포에 특이적으로 많은 발현을 보이는 것을 확인하였다. TTN3가 넉아웃 된 셀에서는 고농도의 포도당 그리고 저삼투압에 의한 양이온 전류, 그리고 세포내 칼슘 유입이 줄어들었고, 분비되는 인슐린의 양도 줄었으며 포도당향상성이 저하 되어있어 정상 쥐에 비해 높은 혈당을 보이는 것을 확인하였다. 본 연구는 기계적 자극 감지 이온채널인 TTN3가 췌장내 베타세포에서 인슐린 분비에 미치는 영향과 분자수준의 메커니즘을 제시하였다.


VERI
LUX
TAS
MEA